Assessment of Drought due to Historic Climate Variability and Projected Future Climate Change in the Midwestern United States

VIMAL MISHRA AND KEITH A. CHERKAUER

Agricultural and Biological Engineering, Purdue University, West Lafayette, Indiana

SHRADDHANAND SHUKLA

Civil and Environmental Engineering, University of Washington, Seattle, Washington

(Manuscript received 2 February 2009, in final form 28 July 2009)

ABSTRACT

Understanding the occurrence and variability of drought events in historic and projected future climate is essential to managing natural resources and setting policy. The Midwest region is a key contributor in corn and soybean production, and the occurrence of droughts may affect both quantity and quality of these crops. Soil moisture observations play an essential role in understanding the severity and persistence of drought. Considering the scarcity of the long-term soil moisture datasets, soil moisture observations in Illinois have been one of the best datasets for studies of soil moisture. In the present study, the authors use the existing observational dataset and then reconstruct long-term historic time series (1916–2007) of soil moisture data using a land surface model to study the effects of historic climate variability and projected future climate change on regional-scale (Illinois and Indiana) drought. The objectives of this study are to (i) estimate changes and trends associated with climate variables in historic climate variability (1916–2007) and in projected future climate change (2009–99) and (ii) identify regional-scale droughts and associated severity, areal extent, and temporal extent under historic and projected future climate using reconstructed soil moisture data and gridded climatology for the period 1916–2007 using the Variable Infiltration Capacity (VIC) model. The authors reconstructed the soil moisture for a long-term (1916–2007) historic time series using the VIC model, which was calibrated for monthly streamflow and soil moisture at eight U.S. Geological Survey (USGS) gauge stations and Illinois Climate Network's (ICN) soil moisture stations, respectively, and then it was evaluated for soil moisture, persistence of soil moisture, and soil temperature and heat fluxes. After calibration and evaluation, the VIC model was implemented for historic (1916–2007) and projected future climate (2009–99) periods across the study domain. The nonparametric Mann–Kendall test was used to estimate trends using the gridded climatology of precipitation and air temperature variables. Trends were also estimated for annual anomalies of soil moisture variables, snow water equivalent, and total runoff using a long-term time series of the historic period. Results indicate that precipitation, minimum air temperature, total column soil moisture, and runoff have experienced upward trends, whereas maximum air temperature, frozen soil moisture, and snow water equivalent experienced downward trends. Furthermore, the decreasing trends were significant for the frozen soil moisture in the study domain. The results demonstrate that retrospective drought periods and their severity were reconstructed using model-simulated data. Results also indicate that the study region is experiencing reduced extreme and exceptional droughts with lesser areal extent in recent decades.

1. Introduction

Climate variability and climate change have been strongly associated with the water and energy cycle and associated extremes, such as drought. Global and regional land surface temperature have increased in the twentieth century and greater warming has been identified in the last three decades (WMO 2005), with 11 of the 12 warmest years observed since 1850 occurring between 1995 and 2006 (Alley et al. 2007). Easterling et al. (1997) conducted an analysis of the global mean surface air temperature and found that because of differential changes between daily maximum and minimum temperatures, the diurnal temperature range is narrowing. Precipitation from 1900 to 2005 has also

Corresponding author address: Vimal Mishra, 225 S. University St., Agricultural and Biological Engineering, Purdue University, West Lafayette, IN 47907.
E-mail: vmishra@purdue.edu

DOI: 10.1175/2009JHM1156.1

increased significantly in the eastern part of North and South America (Alley et al. 2007). The effects have also been observed on the hydrologic cycle and its components as a result of changes in the climate variables, such as precipitation and air temperature.

Lettenmaier et al. (1994) analyzed climate and streamflow data for the continental United States from the period 1948 to 1988 and found (i) an increase in March temperature, (ii) an increase in precipitation from September to December, (iii) an increase in streamflow in the November–April period and (iv) a decrease in temperature range between late spring and winter. The effects of climate variability and change have been observed on other variables as well. For instance, the start of the frost-free season in the northeastern United States has been observed to occur 11 days earlier in the mid-1990s than in the 1950s (Cooter and LeDuc 1995) while peak streamflows associated with snowmelt are also occurring earlier in the year (Regonda et al. 2005; Stewart et al. 2005). Lastly, there has been an observed increase in the number of days with heavy precipitation during the twentieth century (Kunkel et al. 1999).

Many of these trends are expected to persist and even strengthen into the future (e.g., Easterling et al. 2000; Sheffield and Wood 2008; Diffenbaugh et al. 2008). Hayhoe et al. (2007) and Cherkauer and Sinha (2009) found, using the data from the selected global climate models (GCMs), that annual air temperatures are expected to increase and that precipitation is expected to increase in winter [December–February (DJF)] and spring [March–May (MAM)] but decrease in the summer [June–August (JJA)] in the midwestern United States. This will contribute to increased streamflow in winter and spring but also increase the likelihood of low flows and drought in the summer months. Diffenbaugh et al. (2008) found that along with the southwestern United States, the Midwest is projected to have increasingly high hot spot metric values for the late twenty-first century. Furthermore, droughts and their effects on agricultural production and water supplies are and will be among the greatest natural hazards in not only the United States but across the globe (Clark et al. 2008).

A drought is an extreme event that is responsive to changes in climate variables. Analysis of drought over the twentieth century in the United States uncovers a great amount of variability (Dai et al. 2004; Sheffield et al. 2004); for instance, the droughts that occurred in the 1930s and 1950s dominate any long-term trend (Kunkel et al. 1996). Karl et al. (1996) found that there has been no long-term trend in drought for the United States and that areas experiencing excessive wetness appear to be increasing since the 1970s. Andreadis and Lettenmaier (2006) found that for most of the continental United States, the severity of droughts has been reduced as a result of wetter conditions over the last 80 years. Sheffield and Wood (2008) analyzed GCM projections for future climate scenarios and found a projected decrease in soil moisture globally, with an increase in the long-term drought frequency projected for the midlatitude regions of North America.

Drought can lead to significant economic loss and immense pressure to society. In the last three decades, droughts and heat waves caused about $145 billion (U.S. dollars) across the United States (Lott and Ross 2006). Therefore, the need for proactive rather than reactive management is now being underscored (Wilhite et al. 2000). However, the identification of drought events is difficult, as there are several definitions—such as meteorological drought, hydrological drought, and agricultural drought (e.g., Wilhite et al. 2000; Keyantash and Dracup 2002; Dracup et al. 1980)—and varying criteria for estimating the start and the end of drought events. Understanding the need to derive an accurate index that can be applied over a region for a variety of applications, Sheffield et al. (2004) proposed that it may be necessary to include as many as contributing processes as possible. For instance, agricultural drought depends on the temporal variability of precipitation and soil moisture, and the availability of moisture to cover losses from evapotranspiration (ET; Sheffield et al. 2004). There are many drought indices—such as the standardized precipitation index (SPI) and the Palmer drought severity index (PDSI)—used in drought studies (e.g., Mo 2008; Dai et al. 2004), but these are typically focused on a single type of drought or a limited number of data sources. More recently, Shukla and Wood (2008) derived a new hydrological drought index known as standardized runoff index (SRI), which they demonstrated could better identify hydrological drought, especially in the snow-dominated regions.

Drought identification is often hampered by the need for better quality input data (for both observational and model simulated) of precipitation, soil moisture, and runoff, and this has led to the use of output from projects such as the North American Land Data Assimilation System (NLDAS; Mitchell et al. 2004), which was designed to provide accurate land surface initial conditions to GCMs to improve climate forecasts. The offline products have, however, found application in drought monitoring. As for quality observations of soil moisture, the best dataset for the United States comes from the Illinois Climate Network (ICN; Hollinger and Isard 1994). Several studies, including those by Maurer et al. (2002) and Schaake et al. (2004), have found that simulated soil moisture is highly model dependent and that more work must be done to improve the results.

Occurrence and magnitude of drought is directly related to variability in the regional hydrologic cycle. The Midwest region is important for the production of corn and soybean, and recently its importance has grown because of increased use of corn in biofuel production. Considering the importance of agricultural production in this region, there is a growing need to study the linkages of climate variability and change with drought. Therefore, important research questions that need to be answered include the following: (i) What regional trends are associated with climate variables and how these are linked with water fluxes and storage; (ii) how have observed trends in climate variables affected regional-scale drought; and (iii) how are the frequency and extent (both temporal and spatial) of extreme and exceptional droughts likely to change under projections of future regional climate?

We use the Variable Infiltration Capacity (VIC) large-scale hydrology model to simulate soil moisture and runoff conditions at a 1/8° spatial resolution for historic (1916–2007) and future (2009–99) climate. These simulations were at a higher resolution and for a longer period than most previous studies (e.g., Dai et al. 2004; Andreadis et al. 2005; Sheffield and Wood 2008). We have calibrated and evaluated the VIC model against observed monthly streamflow from multiple local U.S. Geological Survey (USGS) gauging stations and individual site observations of soil moisture, whereas previous studies have used only a handful of larger basins and not included soil moisture in their calibration. We have also included the effects of seasonal soil frost on infiltration and soil moisture drainage—something not considered in previous larger-scale studies. This study was designed to address the following objectives: (i) estimate changes and trends associated with climate variables in historic climate variability and in projected future climate change and (ii) identify regional-scale droughts and associated severity, areal extent, and temporal extent under historic and projected future climate using reconstructed soil moisture data from the VIC model.

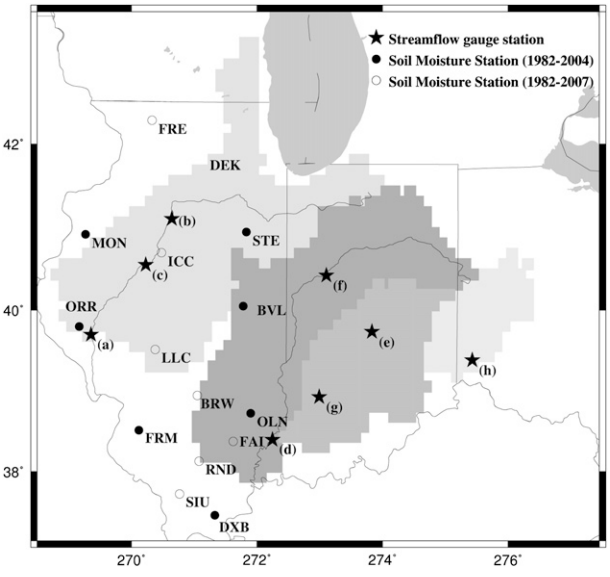

FIG. 1. Location of watersheds, streamflow gauging stations, and soil moisture observation sites used in model calibration and evaluation. Gauging stations in Illinois unless otherwise noted: (a) Illinois River at Valley City; (b) Illinois River at Henry; (c) Illinois River at Kingston Mines; (d) Wabash River at Mt. Carmel; (e) White River at Indianapolis, IN; (f) Wabash River at Lafayette, IN; (g) White River at Newberry, IN; and (h) Miami River at Hamilton, OH. Soil moisture sites include (1) BVL, (2) DXB, (3) BRW,* (4) ORR, (5) DEK, (6) MON, (8) ICC,* (9) LLC,* (10) FRM, (11) Carbondale* (SIU), (12) OLN, (13) FRE,* (14) RND,* (15) STE, and (34) Fairfield* (FAI). Model simulations for the drought analysis were limited to Indiana and Illinois. The asterisk indicates the soil moisture observations used were for 1982–2007; otherwise, observations used were for 1982–2004.

2. Methods and data

a. Study region

This study was conducted in Illinois and Indiana (Fig. 1), an area well known for its agricultural production, especially corn and soybeans. The region consists of the rolling forested landscape in southern Indiana and Illinois, and the much flatter northern and central areas, which are dominated by row crop agriculture (Easterling and Karl 2000). Mean annual daily maximum temperature (based on observations from 1916 to 2007) is 17°C, whereas mean annual daily minimum temperature is 4.8°C. Mean annual precipitation for the study domain is 971 mm. The occurrence of soil freezing in winter and soil thawing in early spring is common, and it affects runoff generation, soil moisture, and flooding. The region drains into the upper Mississippi and Ohio River basins.

b. The VIC model

The Variable Infiltration Capacity model, originally developed jointly at the University of Washington and Princeton University, is a macroscale hydrology model used to simulate water and energy fluxes, including soil moisture and runoff, which are used to estimate drought indices for the study domain. The VIC model (Liang et al. 1994, 1996; Cherkauer and Lettenmaier 1999; Cherkauer et al. 2003) is a physically based model that solves a full energy and water balance for every grid cell. Vegetation is represented using a mosaic scheme in which multiple vegetation types can coexist in a single grid cell. Land cover classes are specified using the leaf area index (LAI), root fraction, canopy resistance, and other parameters. The VIC model is a well-established

large-scale hydrology model (e.g., Abdulla et al. 1996; Lohmann et al. 1998; Nijssen et al. 1997, 2001; Wood et al. 1997; Maurer et al. 2002), and it has well-developed cold-season process routines, such as those for soil frost and snow accumulation and melt (Cherkauer and Lettenmaier 1999; Cherkauer et al. 2003).

The VIC model soil moisture estimates, in particular, have been widely evaluated. Nijssen et al. (2001) found good correlation between observed and simulated soil moisture for stations in Illinois. Maurer et al. (2002) conducted simulations using the VIC model and found that soil moisture persistence is better reproduced by the VIC model than the leaky bucket model of Huang et al. (1996), which is the model used by the National Weather Service's (NWS) Climate Prediction Center (CPC) in its Soil Moisture Monitoring program for the United States (available online at http://www.cpc.noaa.gov/products/Soilmst_Monitoring/). Robock et al. (2003) compared soil moisture from the VIC model to observations from Great Plains mesonet stations and found good agreement. Moreover, the VIC model has been applied to reconstruct historical droughts in many previous studies (e.g., Sheffield et al. 2004; Andreadis et al. 2005; Andreadis and Lettenmaier 2006; Sheffield and Wood 2007; Shukla and Wood 2008). We used the VIC model version 4.1.0 r3 with full energy and water balance, and frozen soils solved using the finite difference soil thermal solution described by Cherkauer and Lettenmaier (1999), with a constant bottom boundary temperature. For all the simulations conducted in this study, the initial 1-yr period was considered as the model spin-up period.

c. *Data*

1) OBSERVED AND PROJECTED CLIMATE DATA

Daily observed climate forcing data included observed daily precipitation, air temperature extremes, and wind speeds. The original precipitation and temperature observations were obtained from the National Climatic Data Center (NCDC) for the period 1915–2007. Daily wind speed data were obtained from the National Centers for Environment Prediction–National Center for Atmospheric Research (NCEP–NCAR) 40-yr Reanalysis project (Kalnay et al. 1996). The wind speed data are available from 1949 and for the period prior to 1949; a daily wind climatology based on the period after 1949 was used (see Hamlet and Lettenmaier 2005). All daily station data were gridded for the study region at a spatial resolution of $\frac{1}{8}°$ (Sinha et al. 2010) using the method of Hamlet and Lettenmaier (2005) to reduce anomalies (or inconsistencies) caused by changes in the number and location of meteorological stations with time. The details about preprocessing, quality control, regridding, temporal adjustment, and topographic adjustments can be found in Hamlet and Lettenmaier (2005).

Projected future climate/meteorological forcing were obtained from GCM simulations developed for the Fourth Assessment Report (AR4) of the Intergovernmental Panel on Climate Change (IPCC). Because there is uncertainty associated with GCM projections, which can be regionally dependent, we used data from three GCMs [third climate configuration of the Met Office United Model (HadCM3.1), Parallel Climate Model version 1.3 (PCM1.3), and Geophysical Fluid Dynamics Laboratory Climate Model version 2.0.1 (GFDL CM2.0.1)] to produce multimodel ensemble statistics for three different scenarios: the Special Report on Emissions Scenarios (SRES) A1B, A2, and B1 (Nakićenović et al. 2000), where the A2 scenario has the highest future emissions of greenhouse gases (GHGs) and B1 has the lowest. These GCMs were selected because they fulfill the criteria described by Cayan et al. (2008) and because they have been used for other studies of regional climate change in the United States, as they provide a range of sensitivities to GHGs and their performance has been deemed acceptable for the Midwest (e.g., Wuebbles and Hayhoe 2004).

Climate projections for all three models and all three scenarios were obtained from the World Climate Research Programme's (WCRP's) Coupled Model Intercomparison Project phase 3 (CMIP3) multimodel dataset. We obtained the CMIP3 data from the Lawrence Livermore National Laboratory (LLNL)–Reclamation–Santa Clara University (SCU) multimodal dataset, stored and served out of the LLNL Green Data Oasis (available online at http://gdo-dcp.ucllnl.org/downscaled_cmip3_projections/dcpInterface.html). These data were bias-corrected using the historic gridded climate forcing dataset using the methodology of Wood et al. (2004), which used an empirical statistical technique to remove biases while preserving the probability density function of the historic monthly data and the future climate trends from the GCM projections. The method was originally developed by Wood et al. (2002) and was later compared successfully with other statistical and dynamic downscaling techniques (Wood et al. 2004). Daily data were disaggregated from bias-corrected monthly totals using daily time series from a monthly historic climatology for the period 1915–2006, in which the selection of historic daily time series for a given month was further refined by sorting historic and future data into wet and dry, and warm and cold climatic periods. As with the historic climatology, the gridded future climate projections included daily precipitation, minimum and maximum daily temperature, and wind speed for 1950 through 2099.

2) SOIL DATA AND LAND COVER DATA

Soil parameters, not reserved for model calibration, were obtained from the Land Data Assimilation System (LDAS; Maurer et al. 2002) at a 1/8° spatial resolution. Vegetation parameters were acquired from the same LDAS dataset. Monthly leaf area index (LAI) data for each vegetation type and each 1/8° grid cell were obtained from Myneni et al. (1997), whereas updated vegetation library parameters (e.g., roughness height, stomatal resistance) were obtained from Mao et al. (2007).

3) SOIL MOISTURE DATA

Soil moisture data were obtained from the Global Soil Moisture Data Bank (Robock et al. 2000) and are described by Hollinger and Isard (1994). These data consist of total soil moisture observations for 19 stations. collected as a part of the Water and Atmospheric Resources Monitoring (WARM) Program run by the state of Illinois. Data obtained from the Global Soil Moisture Data Bank (Robock et al. 2000) cover the period of February 1981 to June 2004, whereas eight sites have continued to collect data past the end of the original project. These data (through 2007) were obtained from R. W. Scott (2008, personal communication), who manages the continuing sites within the ICN. All observations were taken using a neutron probe, with supporting calibration data collected with gravimetric observations. Soil moisture observations were made for the top 10 cm of soil and then at 20-cm intervals to the depth of 2 m. All of the soil moisture observational sites are located in grass except one (Dixon Springs; DXB), which is located in bare soil. We selected 15 soil moisture stations, including 7 with data through 2007, for comparison with model simulations (Fig. 1).

4) FLUX AND SOIL TEMPERATURE DATA

We obtained observations of daily latent heat flux (LHF) and sensible heat flux (SHF), and soil temperature from the Bondville, IL (BVL), AmeriFlux station (available online at http://public.ornl.gov/ameriflux/), located in the central-eastern part of Illinois. Observational data for this site started in 1996, and data collection is ongoing. We used data for the period 1997–2007, as data for 1996 were not available for the entire year. There are two other AmeriFlux sites within the study domain, but the site at Bondville was the only one to include soil temperature, latent heat flux, and sensible heat flux observations; therefore, it is the only site used for model evaluation.

5) MONTHLY STREAMFLOW DATA

Observed monthly streamflow data were obtained for eight gauging stations (Fig. 1) within the study domain, which were operated by the USGS. These data were used to calibrate the VIC model's parameters and to evaluate the effectiveness of those calibrated parameters.

d. Statistical analysis

1) TREND ANALYSIS

To understand the impact of climate variability, the nonparametric Mann–Kendall test was applied using a 5% significance level. This test has been widely used for the detection of trends in hydrologic and climatic data (e.g., Lettenmaier et al. 1994; Kunkel et al. 1999; Yue and Wang 2002; Sinha and Cherkauer 2008), and it is described here in brief.

The Mann–Kendall test identifies a trend without considering if it is linear or nonlinear in a given time series. The test is based on the statistic S, which is defined as

$$S = \sum_{i=1}^{N-1} \sum_{j=i+1}^{N} \operatorname{sgn}(Y_j - Y_i), \tag{1}$$

where Y_j and Y_i are data points in given time series, N is the total number of data points, and

$$\operatorname{sgn}(\alpha) = \begin{cases} 1 & \alpha > 0 \\ 0 & \text{if} \quad \alpha = 0 \\ -1 & \alpha < 0 \end{cases}. \tag{2}$$

A positive (negative) value of S indicates an increasing (decreasing) trend, whereas the significance of the test is estimated using the standardized normal test statistic Z:

$$Z = \begin{cases} \dfrac{(S-1)}{\sqrt{\operatorname{Var}(S)}} & S > 0 \\ 0 & \text{if} \quad S = 0 \\ \dfrac{(S+1)}{\sqrt{\operatorname{Var}(S)}} & S < 0 \end{cases}, \tag{3}$$

which is evaluated in this study using a 5% significance level.

This method was used to estimate trends in the annual average anomalies of precipitation P, maximum air temperature (T-max), minimum air temperature (T-min), total column soil moisture (SM-Total), surface soil moisture (top VIC model layer = top 10 cm; SM-Surf), frozen soil moisture (part of total soil moisture that remains in a frozen condition as ice; SM-Frozen), and total runoff (runoff + baseflow). SM-Total was estimated by dividing the soil moisture of each layer by its respective field capacity and taking the average of the resulting fractional soil moisture. The field capacity values for all three soil layers of each grid cell in the study domain were obtained from the LDAS soil parameter file (see Maurer et al. 2002). This method of calculating total soil moisture was selected because it reduces the bias generated by soil

moisture from the thickest soil layer, which may, in turn, affect the derived trends and variability. For each variable, annual average anomalies were estimated by subtracting the long-term (i.e., 1916–2007) mean value from the annual average values. Snow water equivalent (SWE) trends were also estimated but based on anomalies of total SWE for the winter and spring seasons. Trends for *P*, T-max, and T-min were estimated using the gridded climatology, whereas trends in the other variables were estimated using the VIC model output data. Trend analysis was conducted for the period 1916–2007 for all variables.

Trend analysis was also conducted on observed soil moisture (OSM) data from the ICN stations. To remove the effect of serial correlation on observed soil moisture time series, we used the trend-free prewhitening approach prior to the application of nonparametric Mann–Kendall test as described by Burn et al. (2004). Time series for the top 10 (OSM-Surf) and 90 cm (OSM-90) soil moisture were used to estimate annual anomalies for the period of record: 1982–2004 for eight closed stations and 1982–2007 for the seven operational stations (Fig. 1). Because the second soil layer was set to 80 cm in the calibration, we used the simulated soil moisture from the top two layers, with thicknesses of 10 and 80 cm, respectively, to compare with the observed soil moisture in the top 90 cm. Therefore, for both observed and simulated soil moisture, no normalization of soil moisture was performed.

2) Soil moisture persistence

A serial autocorrelation test was used to estimate persistence (or memory) of the monthly soil moisture anomalies. When the value of the autocorrelation function (ACF) first reaches zero for monthly anomalies of soil moisture variables (e.g., SM-90 and OSM-90), the lag was considered to be the persistence, in months, of soil moisture. Monthly anomalies were estimated by subtracting the long-term (1916–2007) mean monthly value from the mean value for each month.

3) Simulation performance measures

Model performance was estimated during calibration and evaluation using three measures of simulation performance: the Nash–Sutcliffe efficiency (NE; Nash and Sutcliffe 1970), the correlation coefficient (*r*) as described by Ivanov et al. (2004), and the ratio of simulated mean flow to observed mean flow (MF_{ratio}). Equations for these are as follows:

$$\mathrm{NE} = 1.0 - \frac{\sum_{i=1}^{N}(O_i - S_i)^2}{\sum_{i=1}^{N}(O_i - \overline{O})^2}, \tag{4}$$

$$r = \frac{N\sum_{i=1}^{N} S_i O_i - \sum_{i=1}^{N} S_i \sum_{i=1}^{N} O_i}{\sqrt{\left[N\sum_{i=1}^{N} S_i^2 - \left(\sum_{i=1}^{N} S_i\right)^2\right]\left[N\sum_{i=1}^{N} O_i^2 - \left(\sum_{i=1}^{N} O_i\right)^2\right]}}, \tag{5}$$

and

$$\mathrm{MF}_{\mathrm{ratio}} = \frac{\overline{S}}{\overline{O}}, \tag{6}$$

where O_i is observed flow and S_i is model simulated flow for the *i*th month, $\overline{O}$ is mean monthly observed flow, $\overline{S}$ is mean monthly simulated flow, and *N* is the total number of months. NE can take any value from minus infinity to 1, *r* varies between 0 and 1, and MF_{ratio} varies from 0 to positive infinity. In this study, values of NE more than 0.35 and less than 0.50 were considered an indicator of *average* performance, between 0.50 and 0.70 indicated *good* performance, and greater than 0.70 indicated *very good* performance. Similar thresholds for NE are also suggested in Boone et al. (2004) and Oleson et al. (2008). The model performance was considered as good if the *r* was greater than 0.8 and very good if *r* was greater than 0.90. Values of MF_{ratio} indicate the overprediction or underprediction of streamflow, where a value of 1 is perfect prediction. The farther MF_{ratio} gets from 1, the greater the difference between the observed and simulated mean streamflow; therefore, values of MF_{ratio} were considered very good between 0.9 and 1.1, and good between 0.80 and 1.2. Additionally, the model performance was also tested for annual average streamflow for the combined period (1986–2005), with correlation coefficients of more than 0.90 considered an indicator of good performance.

e. Drought indices

Drought periods and drought categories (i.e., exceptional, extreme, severe, and moderate) were estimated using three drought indices: SPI for meteorological drought, SRI for hydrological drought, and SM percentiles for agricultural drought. Here, we describe these indices in brief; refer to Mo (2008) for detailed information.

1) Standardized precipitation index

The deficit in precipitation is measured using the SPI, which is based on the probability of precipitation at different time scales. Developed by McKee et al. (1993, 1995), the SPI has been widely used to identify meteorological drought conditions (e.g., Mo 2008; Shukla and Wood 2008). Drought severity was identified using the ranges described by Svoboda et al. (2002). A drought

TABLE 1. Parameters adjusted during calibration of the VIC model, their range, and the final values selected for the simulations.

Soil parameter	Description	Unit	Range	Value
Bi	Infiltration shape parameter	None	0–0.4	0.1
Ds	Fraction of Dsmax where nonlinear baseflow begins	None	0–1	0.005
Dsmax	Maximum subsurface flow rate	mm day^{-1}	0–30	25
Ws	Fraction of the maximum soil moisture where nonlinear baseflow occurs; Ws > Ds	None	0–1	0.95
D2	Depth of the second soil layer	m	0.1–1.5	0.80
D3	Depth of the third soil layer	m	0.1–1.5	1.0
Expt1	Parameter describing the variation of Ksat with soil moisture in the first layer	None	None	22
Expt2	Parameter describing the variation of Ksat with soil moisture in the second layer	None	None	26

event was classified as an *exceptional* drought if SPI was less than −2.0, an *extreme* drought if SPI was between −1.6 and −1.9, a *severe* drought if SPI was between −1.3 and −1.5, and a *moderate* drought if SPI was between −0.8 and −1.2.

2) STANDARDIZED RUNOFF INDEX

The deficit of runoff is measured using the SRI, which is based on the probability of runoff at different temporal scales. SRI was developed and applied by Shukla and Wood (2008). In this study, the SRI was computed using time series of monthly-mean total runoff rather than streamflow to develop spatially distributed maps, similar to those derived for the SPI. Drought severity for the SRI was identified using the same ranges defined for the SPI.

3) SOIL MOISTURE PERCENTILES

Soil moisture percentiles were estimated using the mean monthly SM-Total. A Weibull plotting position was used to estimate percentiles, as described by Wang et al. (2009) and Andreadis et al. (2005), using the mean monthly soil moisture values for the period 1916–2007. Percentile values less than 20 were considered drought, and the severity of drought was determined based on the definitions of Svoboda et al. (2002). A drought event was classified as an exceptional drought if the soil moisture percentile was less than 2, an extreme drought if it was between 2 and 5, a severe drought if it was between 5 and 10, and a moderate drought if it was between 10 and 20.

f. The VIC model implementation

1) MODEL CALIBRATION AND EVALUATION

Eight USGS gauge stations (Fig. 1) were selected to calibrate the VIC model's soil parameters. Simulated monthly streamflow values were obtained after routing runoff and baseflow from each grid using the method of Lohmann et al. (1996) to locations representing the USGS gauging stations, whereas simulated soil moisture was compared against the observations at individual ICN sites (Fig. 1). Eight soil parameters (Table 1) were adjusted during calibration. The effectiveness of model calibration was checked using visual comparison of the observed and simulated hydrographs as well as annual average monthly soil moisture and also using the statistical performance measures described previously. The first six parameters listed in Table 1 are most influential on runoff and baseflow simulations, whereas the last two parameters have the greatest effect on soil moisture levels (Meng and Quiring 2008).

The model calibration period for streamflow was selected to be the period 1986–95, with evaluation from the period 1996–2005. These periods were selected to minimize the effect of land cover change on streamflow, as we used the LDAS vegetation parameters (Maurer et al. 2002) that represent the year 1992. Performance measures were estimated separately for the calibration period and evaluation. All watersheds were calibrated to use a single set of parameters to simplify the transfer of those parameters to uncalibrated areas. This strategy potentially decreased the quality of the calibration for individual river basins. The VIC model with calibrated soil parameters was then evaluated for monthly streamflow as well as its ability to simulate soil moisture (SM-90, SM-Surf), LHF, SHF, and soil temperature (at 10 cm; ST-10). Soil moisture evaluations were conducted using ICN observations from discrete dates, whereas daily energy fluxes and soil temperatures were obtained from the Bondville, IL, AmeriFlux site.

2) SIMULATIONS FOR HISTORIC AND FUTURE CLIMATE

After calibration and evaluation, the VIC model was implemented for observed historic climate (1916–2007), present-day climate from GCMs (1976–2007), and projected future climate from GCMs (2009–99). In simulations for all periods, soil and vegetation parameters were not modified from those used during the calibration and evaluation, thus limiting changes in hydrology to those resulting from the different climate forcing datasets. All simulations used a 1-yr spin-up period: 1915 for the historic, 1975 for GCM present, and 2008 for the future GCM climate datasets. For the future climate scenarios (B1, A1B, and A2), daily climate forcing for all three climate model projections (PCM, GFDL, and HadCM3)

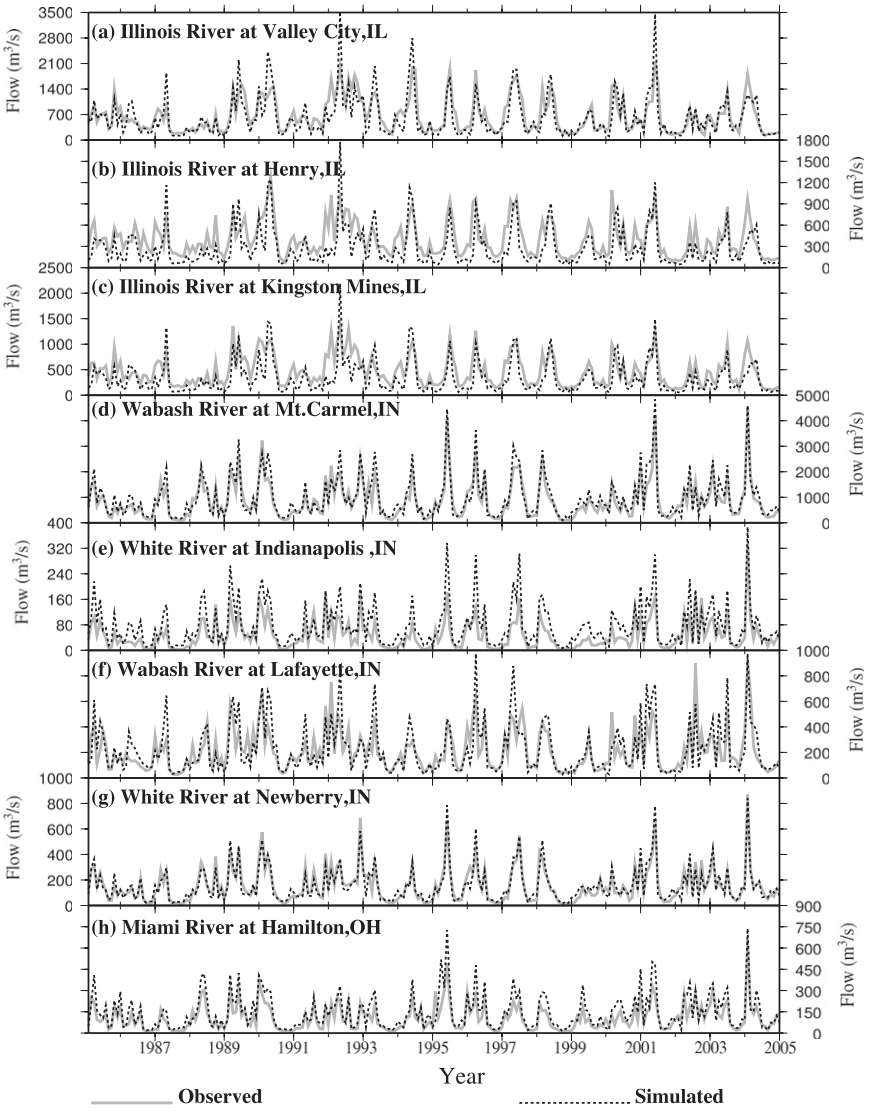

FIG. 2. Model performance for monthly streamflow simulations at the selected USGS gauging stations within the study domain. The period of 1986–1995 was used for model calibration, whereas the1996–2005 period was used for model evaluation.

were used to drive the VIC model independently. All the simulations were conducted using full water and energy balance mode, and with activated frozen soil algorithm (Cherkauer and Lettenmaier 1999).

3. Results

a. Model setup for drought estimation

1) MODEL CALIBRATION AND EVALUATION

The calibration and evaluation of soil parameters resulted in VIC model estimates of annual average monthly streamflow that were in good agreement with observations (Fig. 2), with NE values greater than 0.50 at six gauging stations during the calibration period and at seven gauging stations during evaluation (Table 2). Overall, six of the eight watersheds were good or very good on at least two of the performance criteria during the calibration period, whereas seven watersheds met the same criteria during evaluation. There was no unidirectional bias in simulated streamflow, with two watersheds outside the good range for MF_{ratio} to both the high and low sides. We assume that the nature of this overprediction/underprediction of streamflow will not affect the estimation of drought events because these drought indices (i.e., SPI, SRI or soil moisture percentiles) use relative rather than absolute changes. To evaluate the model's ability to capture year-to-year variability in annual average streamflow,

TABLE 2. Statistical performance of the VIC model during calibration and evaluation periods for the selected gauge stations.

Gauging Station	Calibration (1986–95)			Evaluation (1996–2005)			Total period (1986–2005)
	NE	r	MF_{ratio}	NE	r	MF_{ratio}	r
Illinois River at Valley City, IL	0.63	0.80	0.93	0.74	0.86	0.94	0.96
Illinois River at Henry, IL	0.36	0.74	0.70	0.35	0.80	0.69	0.91
Illinois River at Kingston Mines, IL	0.37	0.75	0.70	0.55	0.84	0.74	0.94
Wabash River at Mt. Carmel, IN	0.83	0.92	1.11	0.90	0.96	1.13	0.95
Wabash River at Lafayette, IN	0.62	0.79	1.07	0.70	0.84	1.05	0.87
White River at Indianapolis, IN	0.53	0.88	1.60	0.60	0.91	1.63	0.92
White River at Newberry, IN	0.88	0.95	0.98	0.90	0.95	1.05	0.94
Miami River at Hamilton, OH	0.73	0.92	1.33	0.66	0.89	1.37	0.95

the correlation coefficient was estimated using simulated annual average streamflow versus observations for the period 1986–2005. Correlation coefficients of greater than 0.90 were found for seven of the eight gauging stations, which indicate that the model is performing well.

2) SOIL MOISTURE SIMULATIONS

Observations of SM-90 from all sites suggest that there is a seasonal cycle associated with soil moisture strongly related to the crop growing period (June–October; Fig. 3), with both observed- and model-simulated SM-90 data

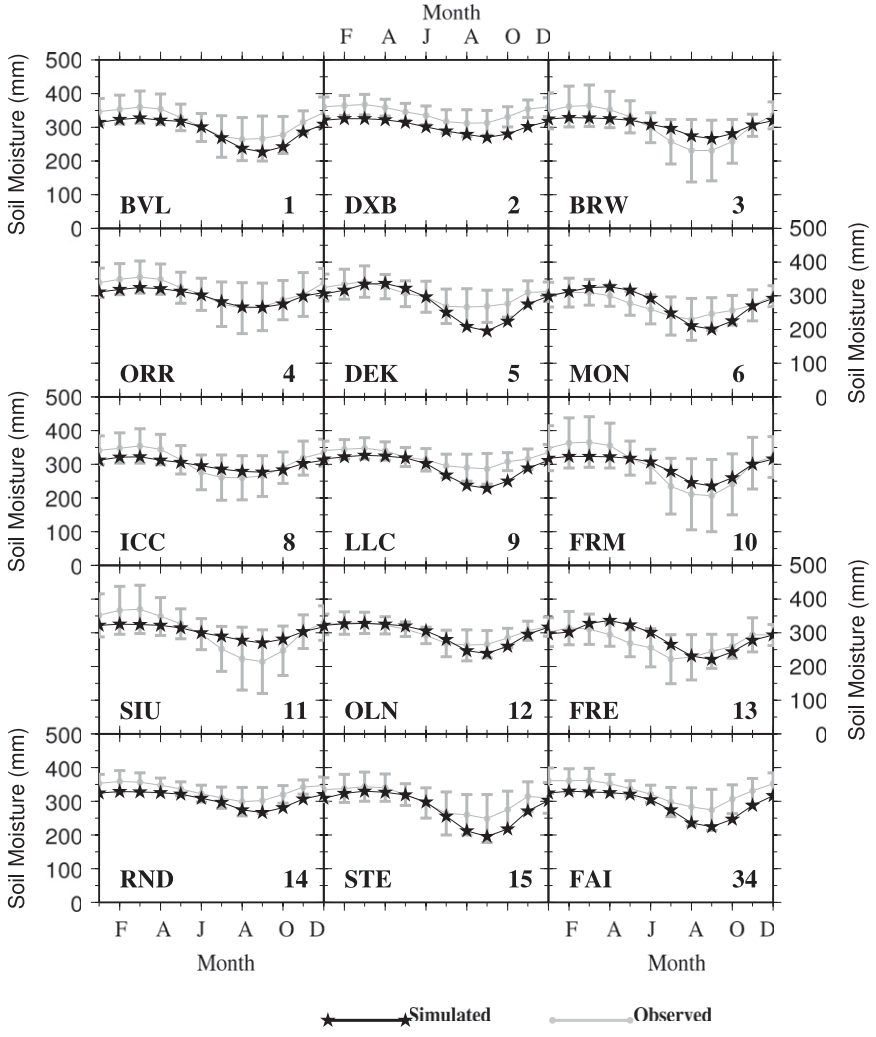

FIG. 3. Mean annual monthly OSM-90 vs SM-90.

TABLE 3. Correlation of annual average monthly VIC model simulated soil moisture vs observations.

Station name	*r*
BVL	0.93
DXB	0.93
BRW	0.97
ORR	0.96
DEK	0.90
MON	0.85
ICC	0.96
LLC	0.92
FRM	0.95
SIU	0.99
OLN	0.92
FRE	0.68
RND	0.92
STE	0.93
FAI	0.95
Median correlation	0.93

experiencing minimum soil moisture values as a result of the higher ET rates. Monthly soil moisture for the DXB station (Fig. 1), which is under bare soil, experienced less seasonal variability than the other ICN stations, as that variability is driven only by precipitation and evaporation (Fig. 3). Correlation coefficients calculated between OSM-90 and SM-90 (Table 3) indicate that simulations are very good at 13 of the 15 sites, with correlation coefficients of more than 0.90 and median correlation for all sites of 0.93. The exceptions include the Monmouth, IL (MON), site, where the *r* is 0.85 and the Freeport, IL (FRE), site, where *r* is 0.68. For both of these ICN stations, SM-90 is higher than OSM-90 during the spring and summer seasons. Earlier studies suggested that the VIC model–simulated soil moisture was close to observations for the composite of ICN stations (Schaake et al. 2004), whereas Nijssen et al. (2001) and Maurer et al. (2002) found that simulated normalized soil moisture showed a significantly low bias. One of the factors contributing to the low bias was found to be the uniform shallow soil depth prescribed by the VIC model in Nijssen et al. (2001). We have improved the VIC model soil parameters in this respect, with D2 now set to 80 compared to 30 cm in both Nijssen et al. (2001) and Maurer et al. (2002), and they do not show an overall low bias.

3) SOIL MOISTURE PERSISTENCE

Persistence, or the autocorrelation of observed- and model-simulated monthly soil moisture anomalies, was computed using the full time series (1982–2004 or 1982–2007, depending on availability of observed data) using lags of 0–10 months in the autocorrelation function (Fig. 5). For most of the stations, simulated and observed soil moisture persistence was on the order of 5–6 months. The model-simulated soil moisture persistence was in a good agreement with observed soil moisture persistence at all the ICN stations (Fig. 4) except one station. Observed soil moisture at the DXB station was significantly more persistent than at any of the other sites, primarily because it is in bare soil. This also led to differences in the magnitude and the range of monthly values of SM-90 (Fig. 4; DXB). These differences can be attributed to the fact that each grid cell was calibrated using the mixed LDAS surface vegetation, which is more closely approximated by the grass sites than the bare soil site, which is why the DXB station is so different. Maurer et al. (2002) used the VIC model to study the persistence of soil moisture anomalies for normalized 1-m soil moisture averaged for all 19 sites in Illinois, and they found that model-simulated anomalies showed lower persistence than observed; however, their analysis used average values for 19 stations, and their model was not calibrated to soil moisture or to as many local watersheds.

4) MODEL PERFORMANCE FOR DAILY SIMULATIONS

Daily values of SM-Surface, ST-10, LHF, and SHF from the VIC model simulation were compared to observations from the BVL AmeriFlux station for the period 1997–2007. Simulated SM-Surf was in a good agreement with both the magnitude and temporal variation of observed daily soil moisture, but the model was most likely underestimating soil moisture in the winter (Fig. 5a). Simulations of ST-10 were also good at predicting the magnitudes of both the seasonal and daily change in temperature (Fig. 5b). The model simulation also captured the annual range and seasonal changes in LHF; however, winter LHF was underpredicted (Fig. 5c). LHF is strongly associated with the type or mixture of vegetation and related parameters; therefore, the more improved representation of vegetation for this particular station might lead to improved model performance. Simulation of SHF (Fig. 5d) agreed well with observations.

b. Climate variability and change

1) HISTORIC TRENDS IN OBSERVED SOIL MOISTURE

The Mann–Kendall trend test analysis was conducted for observed soil moisture (OSM-Surf and OSM-90) anomalies at all 15 of the ICN stations evaluated (Fig. 6). All stations were analyzed for the full period of observation—so, 1982–2004 for the eight closed stations and 1982–2007 for the seven stations still operating. Monthly anomalies were estimated using the available observed data for each station. Significant increasing, increasing but not significant, and decreasing trends were observed in OSM-Surf and OSM-90.

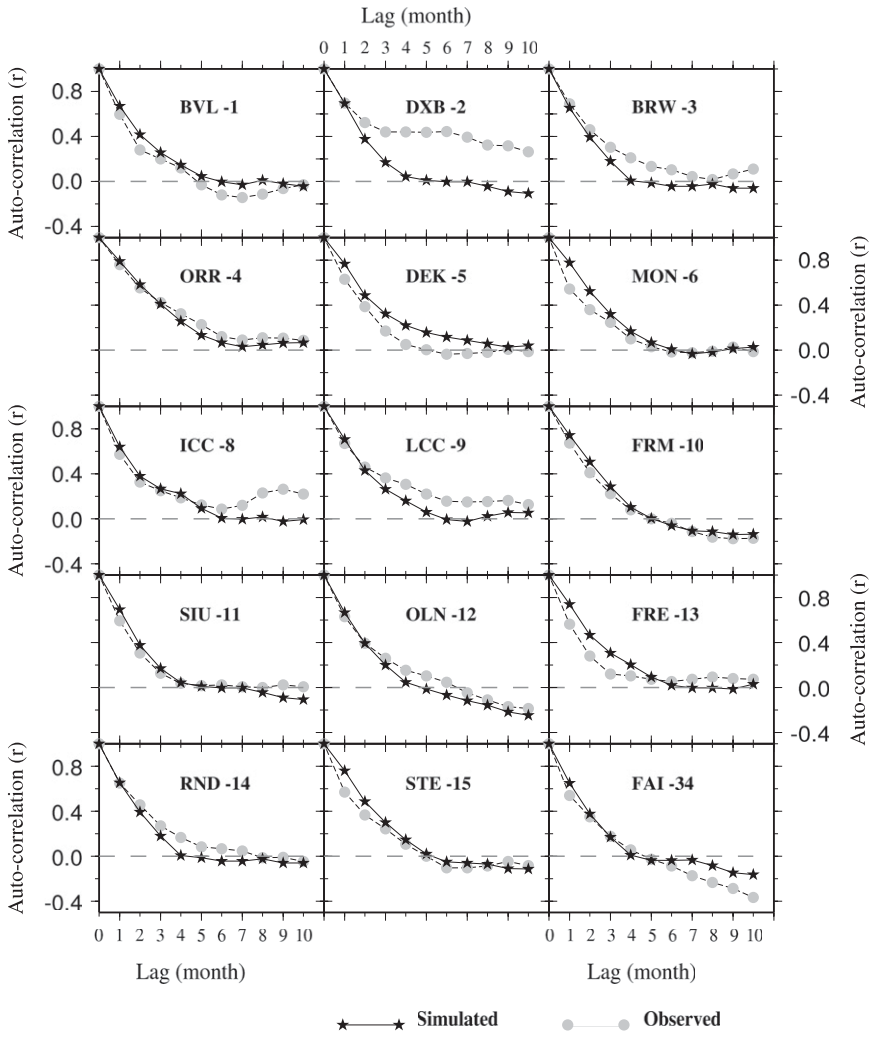

FIG. 4. Autocorrelations estimated using observed- and VIC model–simulated monthly soil moisture anomalies showing the persistence of soil moisture at each site.

Trend analysis for OSM-Surf found that all but two of the sites experienced an upward trend, with the exceptions being MON and Peoria (ICC) in northwestern Illinois. Trends were stronger for stations located in the southern part of the study domain (Fig. 6a). Statistically significant trends (at a 5% significance level) were found at only 4—Brownstown (BRW), Olney (OLN), Rend Lake (RND), and Stelle (STE)—out of 15 stations. All of these were increasing trends, and three of these stations were located in the southern part of the study region.

Four—De Kalb (DEK), ICC, Springfield (LCC) and Belleville (FRM)—out of 15 stations experienced a downward trend for OSM-90 (Fig. 6b), although none of stations was significant. Statistically significant increasing trends were found for four sites—DXB, Orr Center (ORR), OLN, and RND—and as was the case for OSM-Surf, these were mostly located in the southern part of the study region (Fig. 6b). Two of the stations with significant trends in OSM-90—OLN and RND—also had significant upward trends for OSM-Surf.

2) HISTORIC TRENDS IN GRIDDED CLIMATOLOGY AND SIMULATED DATA

Mann–Kendall trend analysis was also conducted on the domain-averaged annual anomalies for the study domain (Fig. 7). An increasing trend, with a slope of 1.13 mm yr^{-1} was identified for domain-averaged precipitation anomalies (Fig. 7a). The daily temperature extremes T-max and T-min experienced decreasing and increasing trends, respectively; however, neither extreme was statistically significant (Figs. 7b,c). SM-Surf experienced a nonsignificant downward trend, whereas SM-Total experienced a significant increasing trend with a slope of 0.19 mm yr^{-1} (Fig. 7f). SM-Frozen had a statistically

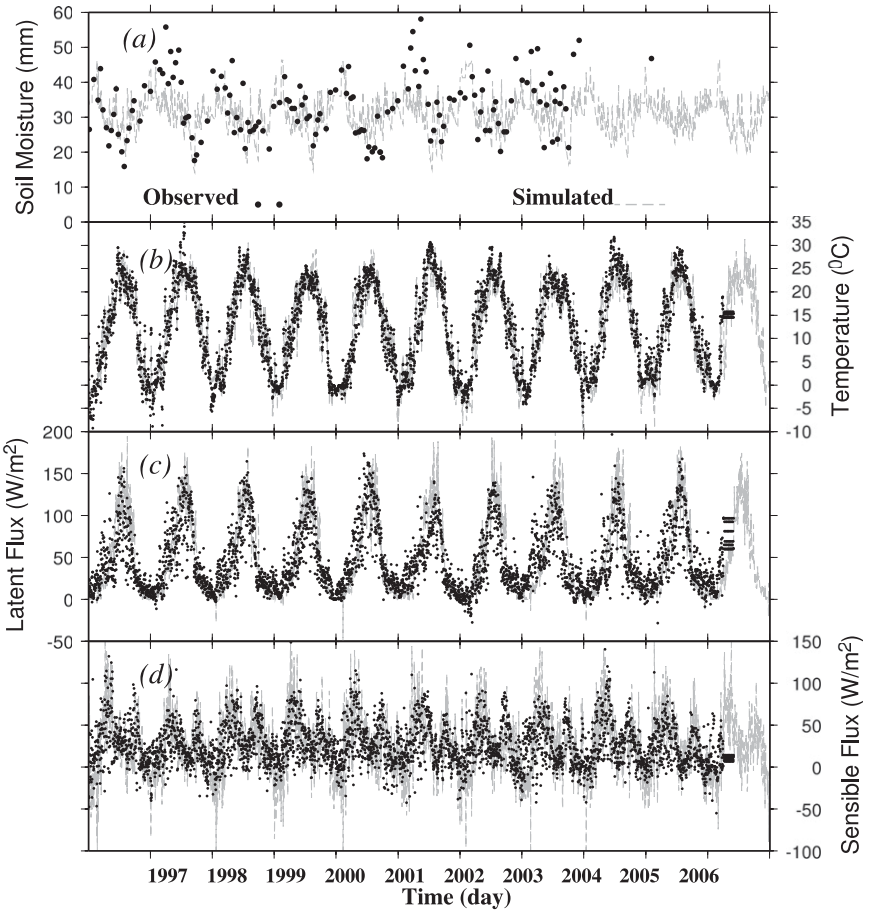

FIG. 5. VIC model–simulated vs daily observations for (a) surface soil moisture, (b) soil temperature at 10-cm depth, (c) latent heat, and (d) sensible heat at the BVL AmeriFlux site.

significant trend with a slope of -0.003 mm yr^{-1} (Fig. 7e), indicating that soil ice has been decreasing. SWE also decreased with a slope of -3.91 mm yr^{-1}, though this was not statistically significant. Total runoff increased significantly, though with a smaller slope (1.11 mm yr^{-1}) than was found for precipitation (1.13 mm yr^{-1}).

To understand these trends and their associated spatial structure, a Mann–Kendall trend analysis was applied to domain-average gridded values of observed meteorology variables (precipitation, T-max, and T-min) and model-simulated variables related to soil moisture snow cover and runoff (Fig. 8). Results demonstrated that there were increasing trends, with slopes of up to 4.0 mm yr^{-1}, associated with precipitation, with a stronger trend in Indiana (Fig. 8a) than in Illinois. Trends in mean annual anomalies of T-max were mostly downward, except for the northern part of Illinois (Fig. 8b). Mean annual anomalies of T-min were found to be increasing for most of the study domain, with slope ranges similar to those of T-max (Fig. 8). These results indicate that the diurnal range of air temperature is narrowing, and they are consistent with the findings of Easterling et al. (1997).

Trends found in SM-Surf reflected the combined effects of trends in precipitation and T-min (Fig. 8d). This suggests that SM-Surf was strongly correlated with T-min in the northern part of the study domain while strongly correlated with precipitation in the central part of Indiana. SM-Frozen was also strongly related to the variation in climatic variables, especially with T-min. Annual anomalies in SM-Frozen were primarily decreasing, most prominently in the northern part of the study domain where colder-season processes are more prominent and susceptible to winter warming (Fig. 8e). Earlier studies demonstrated that, in general, there is a significant difference in the number of frost-free days in both the northern and southern parts of the study domain. For instance, frost-free days in Illinois varied between 160 in the north to more than 190 in the south (Angel 2003). Sinha et al. (2010) also investigated that there is a

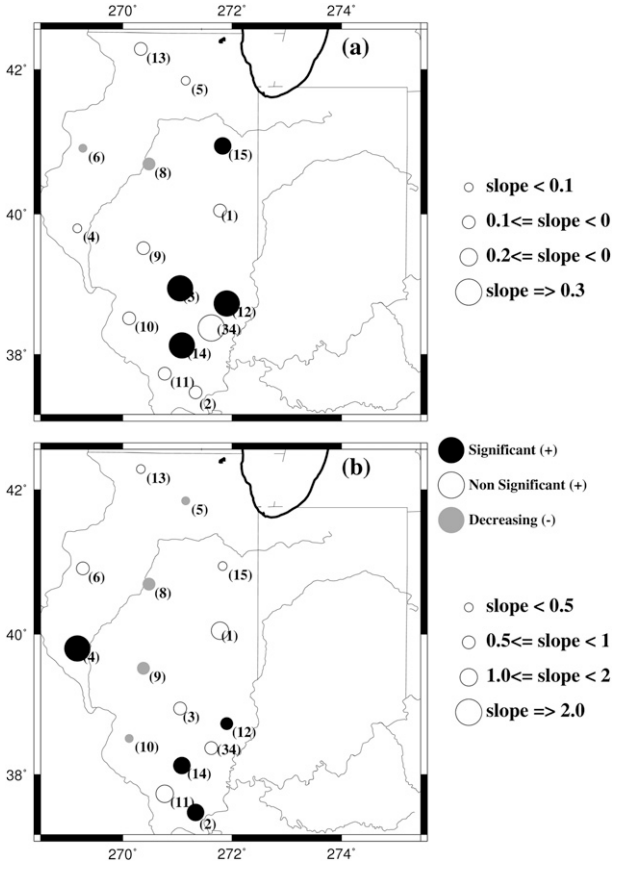

FIG. 6. Trend analysis conducted using observed soil moisture data at selected stations for (a) OSM-Surf and (b) OSM-90. Size of circles represents the magnitude of slope. Black represents significantly increasing trend; gray represents significant decreasing trend; and open circles represent increasing but not significant trends. Trends were estimated using a 5% confidence level.

greater amount of spatial variability among cold-season variables in the study domain. For instance, the number of frost days and frost depth is significantly higher in the northern part comparing to the south part of the study domain. This variability could lead to a weaker magnitude of trend (because the magnitude of SM-Frozen is significantly low in the south) in SM-Frozen and therefore the lower trend on regional average can be attributed to this spatial variability.

Trends for SM-Total reflect the effects of increasing precipitation in Indiana (Fig. 8f). Snow cover, represented by anomalies in annual average SWE, also showed a decreasing trend (Fig. 8g), and as with SM-Frozen, that decline was most significant in the northern part of the domain. Trends associated with total runoff expressed similar patterns to those observed in precipitation, with a more prominent increase in central Indiana (Fig. 8h). Results of historic climate variability highlight that anomaly of precipitation, runoff, T-min, and soil moisture (SM-Total, SM-Surf) have increasing trends, whereas anomaly of T-max, SM-Frozen, and SWE have decreasing trends. The effects of decreasing T-min are more prominent to those regions where a relatively colder winter season is experienced.

3) EFFECTS OF PROJECTED FUTURE CLIMATE CHANGE

Effects of projected future climate change were estimated using the ensemble mean of the VIC model simulations driven using downscaled and bias-corrected climate forcing data from PCM, GFDL, and HadCM3 for emission scenarios A1B, A2, and B1. Differences for mean annual monthly fluxes were estimated by comparing climate scenario ensembles from the project future climate with those from the historic observed climate period.

Projected future climate scenarios indicated a general increase in annual average precipitation, air temperature, and total runoff (Table 4). Mean annual monthly precipitation was projected to increase in winter and spring, whereas it would generally decrease in summer and autumn [September–November (SON); Fig. 9a]. These findings are consistent with the earlier studies (e.g., Cherkauer and Sinha 2009; Hayhoe et al. 2007). Mean annual monthly T-max and T-min were projected to increase in all seasons for all the emission scenarios by 2°–4°C (Figs. 9b,c), with the greatest increases occurring in the summer and early fall.

Results indicate that mean annual monthly SM-Surf was likely to decrease in all seasons, with a more prominent decrease in the winter and spring seasons (Fig. 9d). Mean annual SM-Surf is likely to decrease by 0.5 (1.6%), 0.4 (1.2%), and 0.5 mm (1.6%) for A1B, A2, and B1 scenarios, respectively (Table 5). In the projected future climate change, mean annual monthly SM-Frozen is expected to decrease in winter and spring seasons (Fig. 9e), whereas mean annual SM-Frozen is expected to decrease by 3.3 (49%), 2.2 (33.5%), and 3.0 mm (45.2%) for A1B, A2 and B1 scenarios, respectively (Table 5). Results for mean annual SM-Total suggest that percentage changes for all three scenarios are less than 0.5% (Table 5). Mean annual monthly SWE was projected to decrease in both winter and spring seasons (Fig. 9g), whereas mean annual SWE decreased for all three future emission scenarios (Table 5).

c. *Climate and drought occurrence*

To understand the effects of changes observed under historic climate variability and projected future climate change on the occurrence, severity, and persistence of drought, we used 12-month SPI (SPI-12) and 12-month SRI (SRI-12) values to capture meteorological and hydrologic

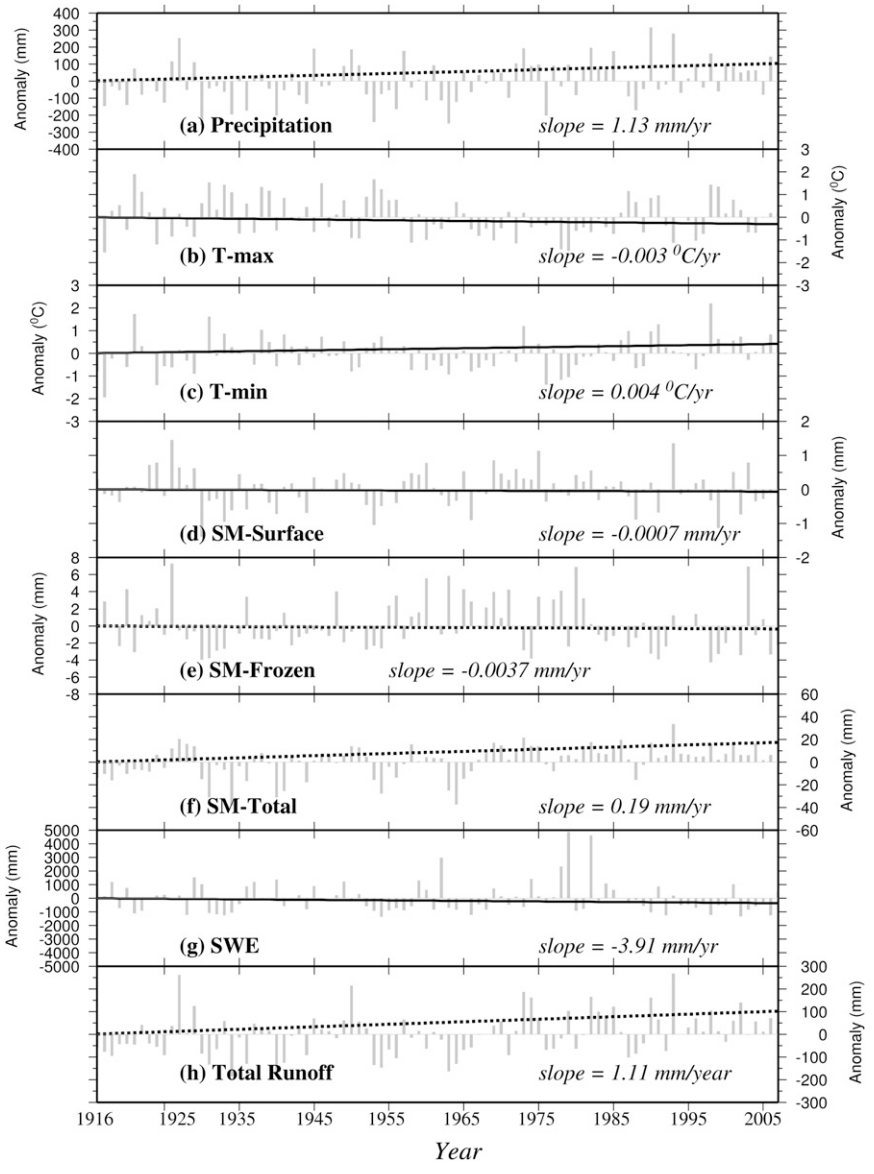

FIG. 7. Trend analysis using annual anomalies of domain-averaged (a) *P*, (b) T-max, (c) T-min, (d) SM-Surf, (e) SM-Frozen, (f) SM-Total, (g) SWE, and (h) total runoff. Dashed lines indicate statistically significant trends at a 5% significance level; solid lines indicate nonsignificant trends.

droughts using observed precipitation forcing and model-derived runoff data for the historic and future simulation periods. These indices were implied to identify major drought periods (periods when drought persisted for at least two years) across the study domain.

DROUGHT IN OBSERVED CLIMATE (1916–2007)

During the observed climate period (1916–2007), major drought spells were identified as 1916–21, 1934–36, 1940–45, 1953–57, 1960–66, 1971/72, 1976/77, and 1987–89 (Table 6). Historic drought events were further categorized into exceptional, extreme, severe, and moderate droughts (Table 6) using the definitions from the Svoboda et al. (2002). All of the most severe and long duration historic drought events were successfully reconstructed (such as droughts in the 1930s, 1940s, and 1950s), which supports the use of the SPI-12 and SRI-12 indices to estimate the frequency of droughts under future climate projections.

The temporal extent of meteorological droughts estimated using SPI-12 for the study domain for early- (1916–45), mid- (1946–75) and late-century (1976–2007) historic periods is shown (Fig. 10). Results suggest that the study domain experienced meteorological drought of

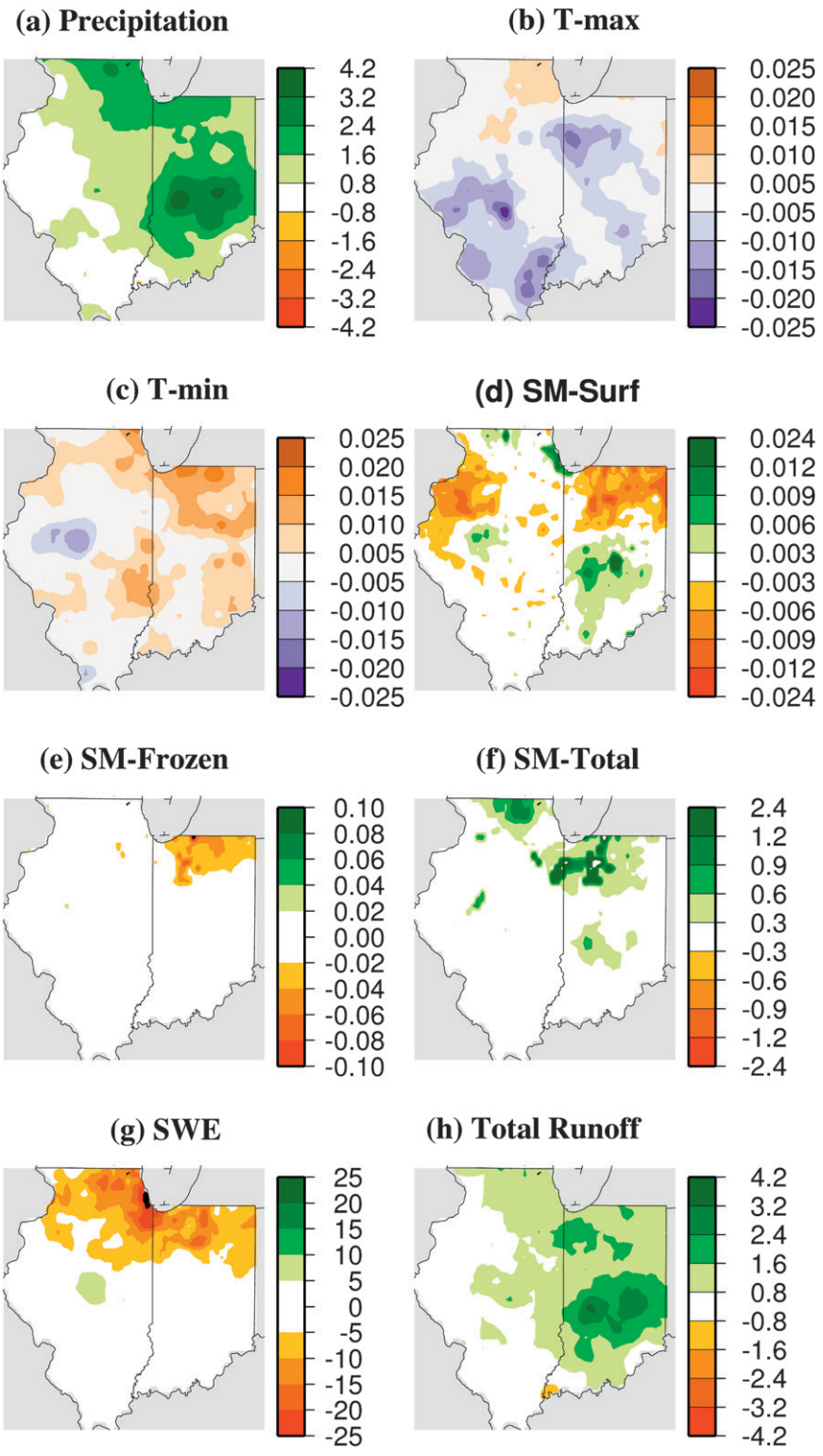

FIG. 8. Slopes of trends from 1916 to 2007 estimated using nonparametric Mann–Kendall test for annual average anomalies of (a) precipitation (significant > 1.02 mm yr^{-1}); (b) T-max (significant < -0.007°C yr^{-1}); (c) T-min (significant > 0.005°C yr^{-1}; (d) SM-Surf (significant > 0.003 mm yr^{-1} and significant < -0.005 mm yr^{-1}); (e) SM-Frozen (significant < -0.03 mm yr^{-1}); (f) SM-Total (significant > 0.3 mm yr^{-1}); (g) SWE (significant < -5 mm yr^{-1}); and (h) total runoff (significant > 0.8 mm yr^{-1}).

TABLE 4. Climatic variables and water balance components for observed and projected future climate. Percentage change in variables for the projected future climate change period is estimated using the ensemble average of three GCMs for three scenarios (A1B, A2 and B1) minus the mean values for the observed period.

Scenario	Precipitation		T-max		T-min		Total runoff	
	Mean (mm)	Change (%)	Mean (°C)	Change (%)	Mean (°C)	Change (%)	Mean (mm)	Change (%)
Observed (1916–2007)	971.2	—	17.0	—	4.8	—	30.6	—
A1B (2009–2099)	1012.6	4.3	19.7	15.8	7.5	57.9	33.3	8.9
A2 (2009–2099)	1004.4	3.4	19.8	16.1	7.7	61.2	32.3	5.7
B1 (2009–2099)	1010.7	4.1	19.2	12.9	7.0	47.6	33.2	8.4

extreme or exceptional categories about 12.5% of the total period of early- and midcentury historic periods, and about 11.3% of the late-century historic period (Fig. 10). These results are consistent with the findings of Andreadis and Lettenmaier (2006) and Karl et al. (1996); they observed that the severity of drought has been reduced because of the wetter conditions over the last 80 years.

Along with the persistence of drought, it is also essential to understand the areal extent of drought events. Monthly areal extent under exceptional and extreme droughts for all three drought indices is presented in Fig. 11 for the historic simulation period. A total of 26 events were identified when meteorological drought (based on the SPI-12) occurred in more than 60% of the study domain, with some of the more prominent meteorological droughts occurring January–April 1931 (more than 90% areal extent), May–July 1934 (more than 92.0%), July–August 1936 (more than 75%), July–October 1940 (more than 60%), March–May 1941 (more than 60%), and October–December 1963 (more than 60%). We identified 19 hydrologic droughts (based on the SRI-12) that occurred over more than 60% of the study domain, including January 1916, March–September 1931 (more than 64%), May–December 1934 (more than 90%), November 1940 (61.0%), and May–September 1941. Lastly, 12 occurrences of extreme and exceptional agricultural droughts (based on SM percentiles) covering more than 60% of the study domain were identified, such as April–May 1931, May–August 1934, July–August 1936, January 1939, March and May 1941, and January and July 1988.

The extent of exceptional and extreme drought conditions was highest for meteorological drought, lower for hydrological drought, and lowest for agricultural drought. This agrees with the relationships between the three indicators, driven by the correlations between precipitation, runoff, and soil moisture, as found by Andreadis et al. (2005). Precipitation and runoff are strongly correlated, whereas the correlation between precipitation and soil moisture is weaker. Therefore, a deficit in precipitation has a stronger influence on runoff deficits than on deficits of soil moisture.

d. Drought in projected future climate (2009–99)

Variability in the projection of major (lasting more than two years) meteorological drought (based on SPI-12) was significant between GCMs and future climate scenarios (Table 7). For instance, under the A1B scenario, the GFDL model projected eight major drought spells, although none of them occurred until 2037; the HadCM3 model projected only four major drought spells more evenly distributed through the next century; and the PCM model projected six major drought periods, mostly early in the next century. The most major drought spells were projected under the A2 scenario, followed by the B1 and A1B scenarios.

The projected duration of exceptional and extreme meteorological droughts in the 30-yr period was estimated using SPI-12 for the study domain and showed a high degree of variability (Fig. 12). Results suggest that the study domain experienced or extreme meteorological droughts about 6% of the last 30 years (1976–2007) based on GCM meteorology for all three climate scenarios (see Fig. 12). Drought duration is projected to decrease in the GFDL model under all scenarios for the next 30 years (2009–38) but increase under the HadCM3 and PCM projections. The midcentury period (2039–68) is projected to be drier for almost all scenarios and models. By the end of the century (2069–99), projections suggest that drought duration will increase under the A2 scenario (highest GHG emissions) but will remain relatively unchanged under the A1B and B1 scenarios.

The meteorological drought index SPI-12 was also used to identify the areal extent of exceptional and extreme droughts under projected future climate (Fig. 13). We notice that there is a model-dependent variability within each emission scenario; however, results indicate that exceptional and extreme drought events covering the 60% or more of the study domain are more likely in the future. Results of this study are consistent with the findings of Sheffield and Wood (2008). Our results also indicate that two of the three climate models under the A1B climate scenario show more exceptional drought events under projected future climate (Table 8).

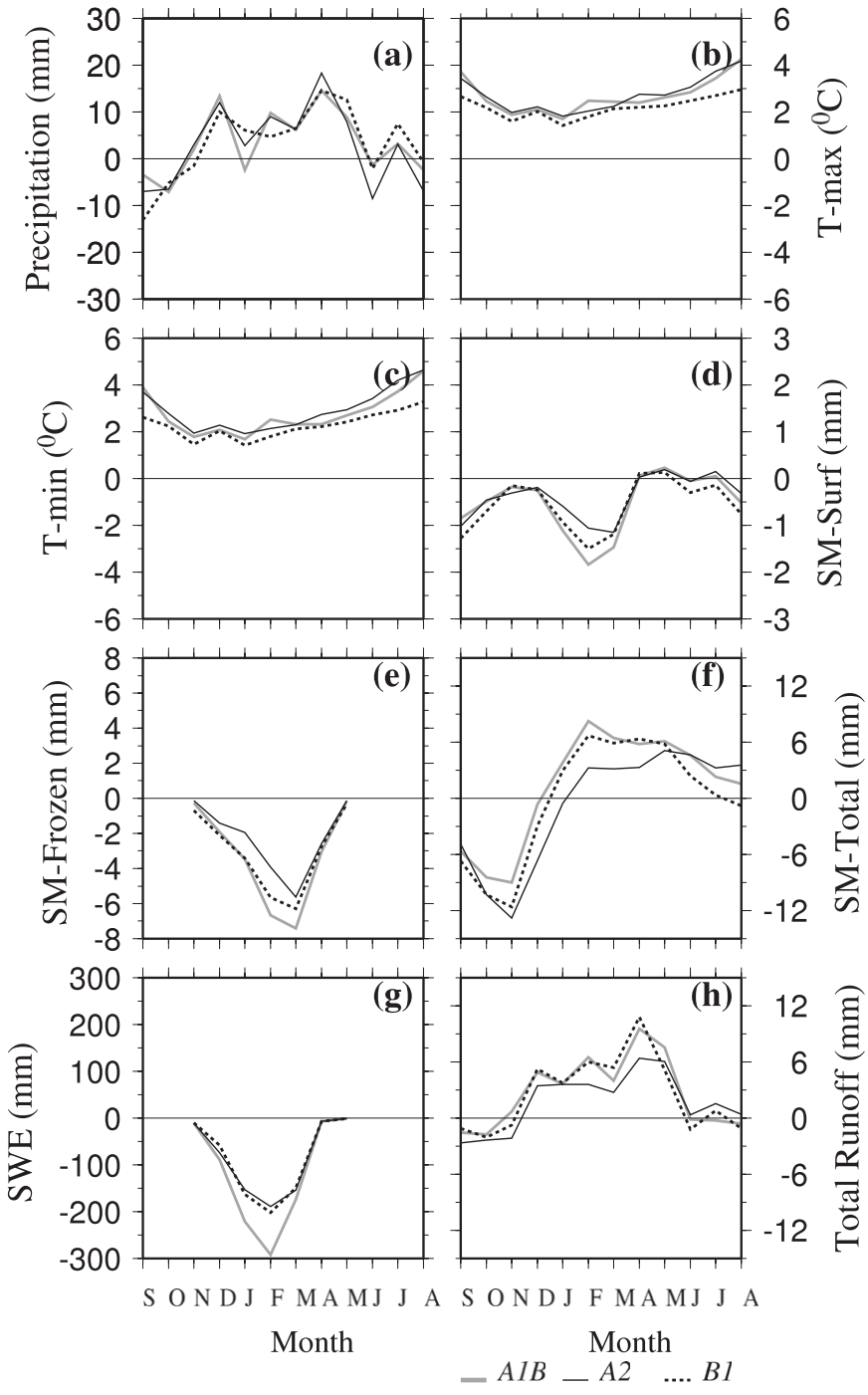

FIG. 9. Mean annual monthly difference estimated using the ensemble average of PCM, GFDL, and HADCM3 for climate scenarios A1B, A2, and B1. Differences were estimated using downscaled and bias-corrected gridded climatologies of (a) precipitation, (b) T-max, and (c) T-min for the period 2009–99 to the observed gridded climatology for the period 1916–2007. For (d) SM-Surf, (e) SM-Frozen, (f) SM-Total, (g) SWE, and (h) total runoff, differences were estimated using VIC model simulations for historic and projected climate scenarios. In each case, differences were estimated by subtracting the historic period from the projected climate period.

TABLE 5. Mean and percent change for soil moisture variables and SWE for observed and projected future climate periods.

Scenario	SM-Surface (mm)		SM-Frozen (mm)		SM-Total (mm)		SWE (mm)	
	Mean (mm)	Change (%)	Mean (mm)	Change (%)	Mean (mm)	Change (%)	Mean (mm)	Change (%)
Observed (1916–2007)	32.8	—	6.7	—	436.0	—	227.5	—
A1B (2009–2099)	32.3	−1.6	3.4	−48.9	437.3	0.3	114.1	−49.9
A2 (2009–2099)	32.4	−1.2	4.5	−33.5	435.3	−0.2	143.2	−37.0
B1 (2009–2099)	32.3	−1.8	3.7	−45.2	435.9	0.0	143.2	−37.0

4. Discussion

Results indicated that Indiana and Illinois have been experiencing significant changes associated with observed climate. Annual precipitation has increased largely in the eastern and central parts of the Midwest, affecting most of Indiana. This is consistent with other studies (e.g., Alley et al. 2007; Groisman et al. 2004; Kunkel et al. 1999) that have found an increase in total and extreme precipitation across the United States. Our results also suggest that in the northern part of the domain where cold-season processes are most significant, SWE is declining. The increase in precipitation and the decline of SWE is an indicator that more precipitation is falling as rain, and that the duration of snow on the ground is decreasing, which is consistent with the findings of Feng and Hu (2007), who found decreasing trends in snowfall across the United States. Increased precipitation can mask the effects of warmer air temperatures on water losses to the atmosphere. For example, Easterling et al. (2007) found that the expected increase in drought occurrence due to increased air temperature was largely nullified by increases in precipitation. Our analysis of trends in historic conditions within the study area indicate a decrease in the variability of daily air temperatures, with T-max decreasing and T-min increasing over the last 91 years, and that coupled with an increase in precipitation results in an increase in simulated total soil moisture and runoff (see Fig. 9). Increasing trends in T-min were also found to have an effect on the occurrence of ice in the surface soil layer, especially in the northern part of the domain where SWE is highly affected, which is consistent with earlier studies (see Sinha and Cherkauer 2008; Cooter and LeDuc 1995. Such trends in hydrologic variables suggest that the frequency and occurrence of drought should be decreasing in the study domain; however, how increased wetness will affect agricultural production depends more on the timing of drought conditions than on their severity or duration. For example, Goldblum (2009) found that corn yields are negatively correlated to July and August temperature and positively correlated with July and August precipitation, so corn yields would be severely affected if drought occurs for even a short time in the summer season.

Evaluation of our simulations indicated that major drought events were successfully reconstructed using the selected drought indices. The noteworthy aspect of the findings was that exceptional drought occurred in almost every decade, starting from Dust Bowl in 1930s through the 1960s (Table 7), after which no drought

TABLE 6. Major drought periods and years with categorical drought occurrence estimated using SPI-12 and SRI-12 for the observed climate period (1916–2007).

Drought periods	Moderate	Severe	Extreme	Exceptional
1916–21	1916	1918	1920	1930
1934–36	1917	1955	1923	1931
1940–45	1919	1966	1925	1934
1953–57	1921	1972	1956	1935
1960–66	1926	1989	1971	1936
1971/72	1942	1992	1976	1940
1976/77	1944	2000	1977	1941
1987/89	1945	2005	1987	1953
	1957		1988	1954
	1960			1963
	1961			1964
	1962			
	1981			
	2003			

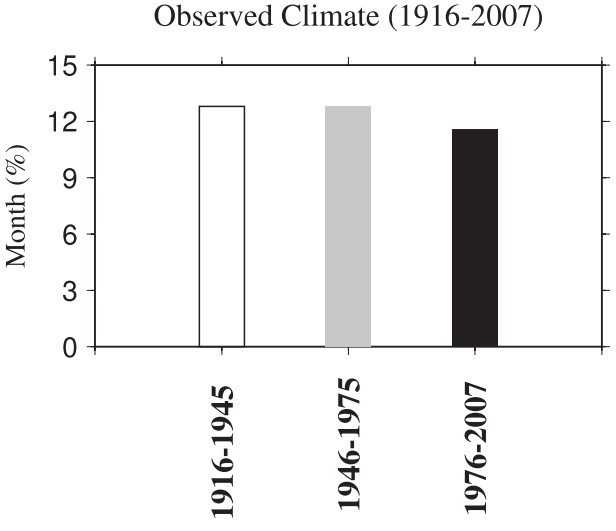

FIG. 10. Percentage of 30-yr period under exceptional and extreme droughts estimated using SPI-12 for observed climate periods representing the early, middle, and late centuries.

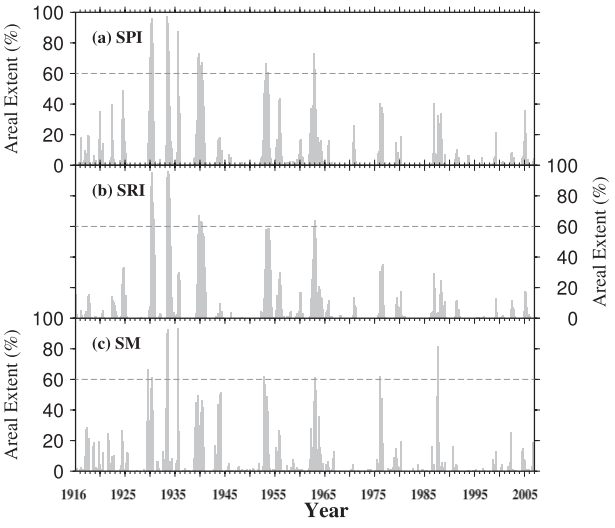

FIG. 11. Monthly areal extent (%) of exceptional and extreme (a) meteorological drought based on SPI-12, (b) hydrological drought based on SRI-12 and (c) agricultural drought based on SM percentiles. A dashed line shows droughts that covered more than 60% of the study domain.

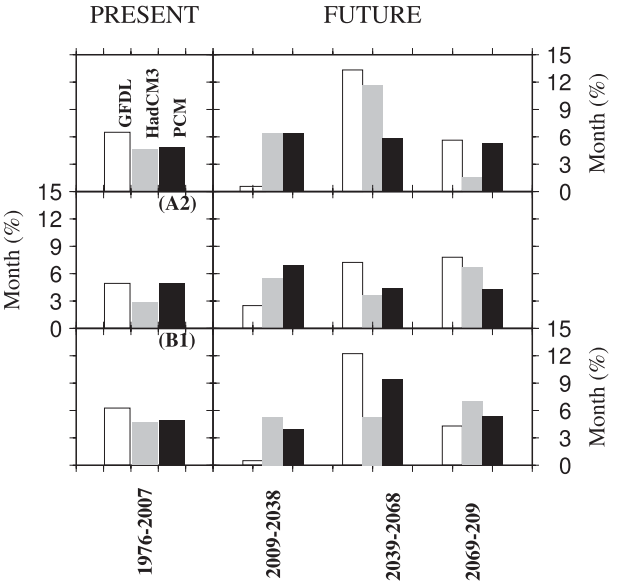

FIG. 12. Percentage of 30-yr climate periods under exceptional and extreme droughts estimated using SPI-12 for the present, and early, middle, and late parts of the current century. All percentages based on downscaled and bias-corrected GCM projections for climate change scenarios A1B, A2, and B1.

events fell into the exceptional category. The most recent extreme drought occurred in 1988, which was the costliest drought in the United States (Riebsame et al. 1991), as it directly affected the study region during the crop growing season. The most recent severe drought occurred in the year 2005 and ranks among the top three most costly in Illinois over the last 112 years (Kunkel et al. 2006), as it also occurred in the crop growing season. Although the occurrence of drought has been a common phenomenon in the study domain, our findings suggest that the occurrence of exceptional and extreme drought has been reduced greatly since 1970 (Fig. 10), as suggested by the observed increasing trend in precipitation. This decreasing tendency for drought within the study domain is consistent with the findings of Karl et al. (1996), Andreadis et al. (2005), and Andreadis and Lettenmaier (2006). This study also found that the areal extent of exceptional and extreme droughts has decreased in recent decades (Fig. 11). Both the decrease in extreme and exceptional drought frequency, and spatial extent should be a benefit to agricultural production, but the economic effect is dependent on the timing of the drought with respect to the growing season and its actual physical extent versus crop distributions. Damage to crops may also not be limited to extreme and exceptional drought levels and so such analysis is left for the future.

Soil moisture, precipitation, and runoff were projected to increase within the study domain as a result of future climate changes (Fig. 9), which is consistent with observed trends under historic climate (1916–2007). The major difference was in T-max, which showed a decreasing trend (not statistically significant) in the observed

TABLE 7. Major multiyear droughts estimated using SPI-12 and SRI-12 for the projected future climate period (2009–2099).

A1B			A2			B1		
GFDL	HADCM3	PCM	GFDL	HADCM3	PCM	GFDL	HADCM3	PCM
2038–44	2018–21	2013–15	2021–23	2012–14	2012–14	2015–18	2009–15	2009–12
2046–48	2023–27	2021–25	2031–33	2017–20	2019–23	2032–34	2023–26	2020–23
2053–55	2045–58	2027–36	2040–42	2022–26	2032–35	2039–44	2031–34	2038–50
2059–61	2088–92	2047–52	2062–64	2028–31	2038–42	2047–49	2057–59	2052–56
2065–69		2070–72	2066–72	2033–35	2047–49	2051–54	2065–69	2060–62
2076–83		2076–83	2075–78	2040–45	2064–67	2064–67	2072–74	2074–78
2085–86			2082–87	2067–69	2072–74	2092–96	2083–85	2080–82
2095–96				2074–77	2081–83			2087–91
					2085–89			

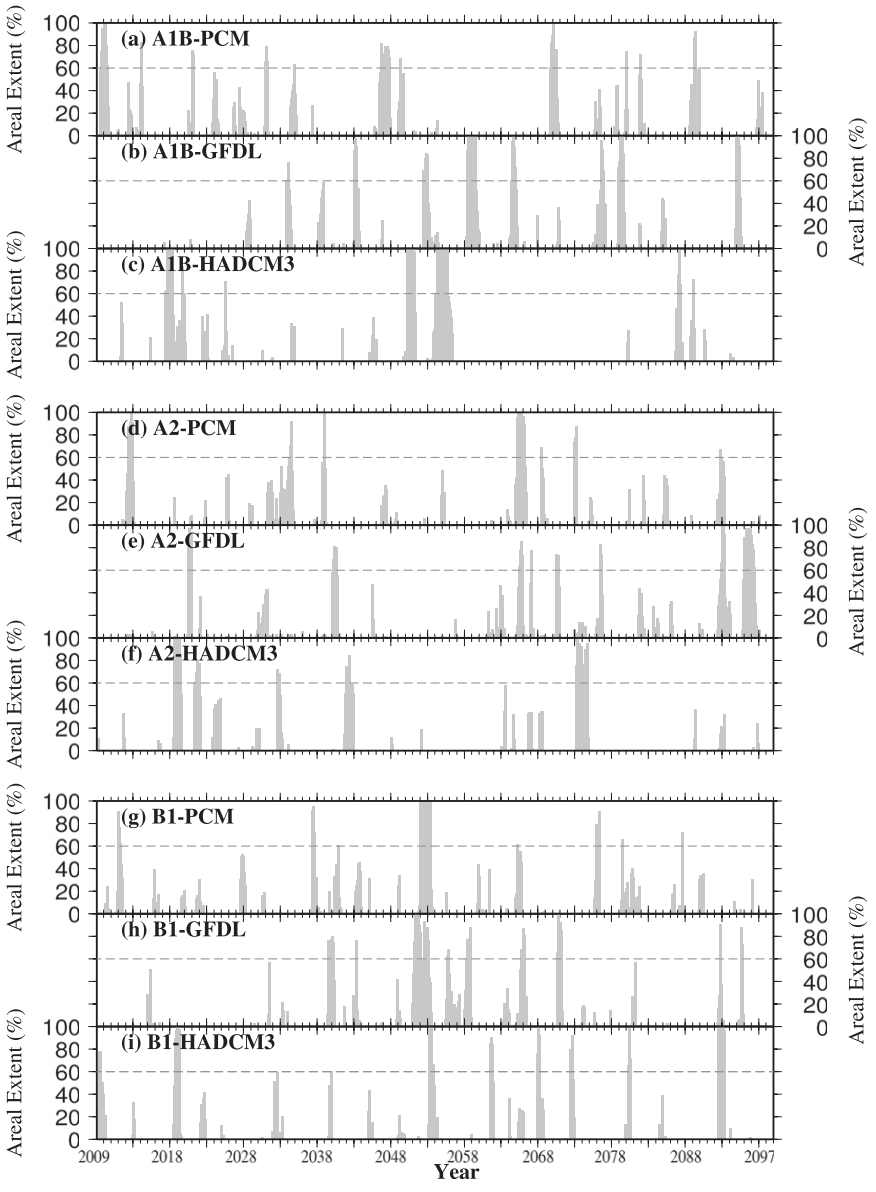

FIG. 13. Monthly areal extents (%) of exceptional and extreme droughts under projected future climate based on the SPI-12 index: (a) PCM and (b) GFDL models under A1B scenario; (c) HadCM3 model under A1B scenario; (d) PCM, (e) GFDL, and (f) HadCM3 models under A2 scenario; and (g) PCM, (h) GFDL, and (i) HADCM3 models under B1 scenario.

climate, but it was projected to increase in the future. With both T-min and T-max projected to increase in the future, water loss to the atmosphere through evapotranspiration should also increase, affecting the occurrence of droughts. Such an increase in the number of months in drought within a 30-yr period was only found for the midcentury period (2039–68), whereas by the end of the century an increase in drought occurrence was only found under the A2 scenario (highest GHG emissions). The spatial extent of such droughts is also projected to affect more than 60% of the study domain on a regular basis, suggesting that in the future, droughts may become more regional in nature than they have been in the recent past. These findings are consistent with the findings of Sheffield and Wood (2008).

5. Summary and conclusions

We used observations of streamflow from USGS gauging stations and soil moisture from the Illinois Climate Network (ICN) to calibrate the Variable Infiltration Capacity (VIC) large-scale hydrology model. Model simulations

TABLE 8. Years with exceptional drought occurrence estimated using SPI-12 and SRI-12 for the future climate period (2009–2099).

A1B			A2			B1		
GFDL	HADCM3	PCM	GFDL	HADCM3	PCM	GFDL	HADCM3	PCM
2035	2018	2009	2021	2009	2013	2040	2009	2011
2044	2019	2010	2041	2019	2014	2041	2019	2012
2053	2020	2022	2066	2020	2035	2052	2020	2038
2059	2051	2032	2068	2022	2039	2053	2054	2052
2060	2052	2047	2077	2023	2066	2054	2062	2053
2065	2055	2048	2094	2043	2067	2059	2069	2054
2066	2056	2050	2097	2074	2073	2066	2073	2076
2077	2088	2070	2098	2075	2074	2067	2081	2077
2079		2071			2093	2071	2093	2081
2080		2080				2072	2094	
2095		2082				2093		
2096		2090				2096		

were further evaluated against estimates of soil moisture persistence, soil temperature, and heat fluxes from available observational datasets. Both observations and model simulations were used to understand the effects of historic climate (1916–2007) variability on drought occurrence. Additionally, we used the calibrated VIC model to understand the severity and variability of drought under observed (1916–2007) and projected future climate (2009–99). On the basis of this study, the following conclusions were made.

Simulated values of soil moisture in the top 90 cm (SM-90) captured the magnitude and variability of observations of soil moisture over the same depth (OSM-90) at stations in the ICN. It was also observed that SM-90 and OSM-90 displayed similar patterns of seasonal changes related to the influence of vegetation.

Persistence of SM-90 as simulated by the VIC model was in a good agreement with observations, with a slight underprediction at 5 of the 15 sites. Results also indicated that there was spatial variability associated with the persistence of individual stations, which might be due to variability of soils, vegetation, topographic features, and climate variables. Statistically significant trends were found in long-term observations of precipitation and in simulated soil moisture and total runoff. Precipitation is increasing while variability in air temperature is decreasing as T-min has been increasing and T-max decreasing. Soil frost (SM-Frozen) and SWE are decreasing in response to the increase in T-min.

Under projected future climate, our results indicate that precipitation T-max and T-min are likely to increase. There is also a likelihood that frozen soil moisture (SM-Frozen) and SWE will follow the same decreasing trend under the projected future climate because of increased air temperature. Total column soil moisture and total runoff are likely to increase with the projected increase in precipitation, offsetting changes in regional air temperature. However, projections suggest that summers will be drier, with most of the extra precipitation falling in winter and spring.

Results demonstrated that the major historical drought events were successfully identified and reconstructed using the model simulations. Additionally, our results indicate that under projected future climate scenarios, the duration of drought is likely to be about the same as in the last 30 years, except for under the A2 scenario (highest emission scenario evaluated), where there is the potential for a small increase in drought duration by the end of the current century. The persistence related to exceptional and extreme drought events is likely to continue to decrease in the future climate, and the frequency of such drought events is likely to increase. Results also suggest that exceptional and extreme drought events occupying 60% or more of the study domain are likely to increase. The findings of this study suggest that further analysis is required to determine the actual effect of future droughts on agriculture and water availability, by studying the seasonality of droughts and their spatial extent versus crop production maps.

Acknowledgments. We acknowledge the review and insightful comments from Dr. Matt Huber, which certainly helped to increase the quality of the present work. We also acknowledge the support of R. W. Scott, who provided recent soil moisture observations. The data availability from the AmeriFlux network is greatly appreciated. Lastly, we are grateful to three anonymous reviewers whose insightful and critical comments greatly helped to improve this manuscript. This project was supported through a grant from the NASA Land Use

Land Cover program (Grant NNG06GC40G) and a graduate fellowship through the Purdue Climate Change Research Center (PCCRC). This is the PCCRC paper 0905.

REFERENCES

Abdulla, F. A., D. P. Lettenmaier, E. F. Wood, and J. A. Smith, 1996: Application of a macroscale hydrologic model to estimate the water balance of the Arkansas-Red River Basin. *J. Geophys. Res.,* **101,** 7449–7459.

Alley, R. B., and Coauthors, 2007: Summary for policymakers. *Climate Change 2007: The Physical Science Basis,* S. Solomon et al., Eds., Cambridge University Press, 1–18.

Andreadis, K. M., and D. P. Lettenmaier, 2006: Trends in 20th century drought over the continental United States. *Geophys. Res. Lett.,* **33,** L10403, doi:10.1029/2006GL025711.

——, E. A. Clark, A. W. Wood, A. F. Hamlet, and D. P. Lettenmaier, 2005: Twentieth-century drought in the conterminous United States. *J. Hydrometeor.,* **6,** 985–1001.

Angel, J. R., 2003: Snow rollers in Illinois. *Bull. Ill. Geogr. Soc.,* **45,** 31–33.

Boone, A., and Coauthors, 2004: The Rhône-Aggregation Land Surface Scheme intercomparison project: An overview. *J. Climate,* **17,** 187–208.

Burn, D. H., J. M. Cunderlik, and A. Pietroniro, 2004: Hydrological trends and variability in the Liard River basin. *Hydrol. Sci. J.,* **49,** 53–67.

Cayan, D., E. Maurer, M. Dettinger, M. Tyree, and K. Hayhoe, 2008: Climate change scenarios for the California region. *Climatic Change,* **87,** 21–42.

Cherkauer, K. A., and D. P. Lettenmaier, 1999: Hydrologic effects of frozen soils in the upper Mississipi River basin. *J. Geophys. Res.,* **104,** 19 599–19 610.

——, and T. Sinha, 2009: Hydrologic impacts of projected future climate in the Lake Michigan Region. *J. Great Lakes Res.,* in press.

——, L. C. Bowling, and D. P. Lettenmaier, 2003: Variable infiltration capacity cold land process model updates. *Global Planet. Change,* **38,** 151–159.

Clark, P. U., and Coauthors, 2008: Abrupt climate change. U.S. Geological Survey Synthesis and Assessment Product 3.4, 459 pp.

Cooter, E. J., and S. K. LeDuc, 1995: Recent frost date trends in the north-eastern USA. *Int. J. Climatol.,* **15,** 65–75.

Dai, A., K. E. Trenberth, and T. Qian, 2004: A global dataset of Palmer drought severity index for 1870–2002: Relationship with soil moisture and effects of surface warming. *J. Hydrometeor.,* **5,** 1117–1130.

Diffenbaugh, N. S., F. Giorgi, and J. S. Pal, 2008: Climate change hotspots in the United States. *Geophys. Res. Lett.,* **35,** L16709, doi:10.1029/2008GL035075.

Dracup, J. A., K. S. Lee, and E. G. Paulson, 1980: On the definition of droughts. *Water Resour. Res.,* **16,** 297–302.

Easterling, D. R., and T. R. Karl, 2000: Potential consequences of climate variability and change for the Midwestern United States. Climate change impacts on the United States: The potential consequences of climate variability and change, National Assessment Synthesis Team Rep., Cambridge University Press, 22 pp.

——, and Coauthors, 1997: Maximum and Minimum Temperature Trends for the Globe. *Science,* **277,** 364–367.

——, J. L. Evans, P. Ya. Groisman, T. R. Karl, K. E. Kunkel, and P. Ambenje, 2000: Observed variability and trends in extreme climate events: A brief review. *Bull. Amer. Meteor. Soc.,* **81,** 417–425.

——, T. W. R. Wallis, J. H. Lawrimore, and R. R. Heim Jr., 2007: Effects of temperature and precipitation trends on U.S. drought. *Geophys. Res. Lett.,* **34,** L20709, doi:10.1029/2007GL031541.

Feng, S., and Q. Hu, 2007: Changes in winter snowfall/precipitation ratio in the contiguous United States. *J. Geophys. Res.,* **112,** D15109, doi:10.1029/2007JD008397.

Goldblum, D., 2009: Sensitivity of Corn and Soybean Yield in Illinois to Air Temperature and Precipitation: The Potential Impact of Future Climate Change. *Phys. Geogr.,* **30,** 27–42.

Groisman, P. Y., R. W. Knight, T. R. Karl, D. R. Easterling, B. Sun, and J. H. Lawrimore, 2004: Contemporary changes of the hydrological cycle over the contiguous United States: Trends derived from in situ observations. *J. Hydrometeor.,* **5,** 64–85.

Hamlet, A. F., and D. P. Lettenmaier, 2005: Production of temporally consistent and gridded precipitation and temperature fields for the continental United States. *J. Hydrometeor.,* **6,** 330–336.

Hayhoe, K., and Coauthors, 2007: Past and future changes in climate and hydrologic indicators in the Northeast. *Climate Dyn.,* **28,** 381–407.

Hollinger, S. E., and S. A. Isard, 1994: A soil moisture climatology of Illinois. *J. Climate,* **7,** 822–833.

Huang, J., H. M. van den Dool, and K. P. Georgarakos, 1996: Analysis of model-calculated soil moisture over the United States (1931–1993) and applications to long-range temperature forecasts. *J. Climate,* **9,** 1350–1362.

Ivanov, V. Y., E. R. Vivoni, R. L. Bras, and D. Entekhabi, 2004: Preserving high-resolution surface and rainfall data in operational-scale basin hydrology: A fully-distributed physically-based approach. *J. Hydrol.,* **298,** 80–111.

Kalnay, E., and Coauthors, 1996: The NCEP/NCAR 40-Year Reanalysis Product. *Bull. Amer. Meteor. Soc.,* **77,** 437–471.

Karl, T. R., R. W. Knight, D. R. Easterling, and R. G. Quayle, 1996: Indices of climate change for the United States. *Bull. Amer. Meteor. Soc.,* **77,** 279–292.

Keyantash, J., and J. A. Dracup, 2002: The quantification of drought: An evaluation of drought indices. *Bull. Amer. Meteor. Soc.,* **83,** 1167–1180.

Kunkel, K. E., S. A. Changnon, B. C. Reinke, and R. W. Arritt, 1996: The July 1995 heat wave in the Midwest: A climatic perspective and critical weather factors. *Bull. Amer. Meteor. Soc.,* **77,** 1507–1518.

——, K. Andsager, and D. R. Easterling, 1999: Long-term trends in extreme precipitation events over the conterminous United States and Canada. *J. Climate,* **12,** 2515–2527.

——, and Coauthors, 2006: The 2005 Illinois drought. Illinois state water survey, 80 pp.

Lettenmaier, D. P., E. F. Wood, and J. R. Wallis, 1994: Hydro-climatological trends in the continental United States, 1948–88. *J. Climate,* **7,** 586–607.

Liang, X., D. P. Lettenmaier, E. F. Wood, and S. J. Burges, 1994: A simple hydrologically based model of land surface water and energy fluxes for general circulation models. *J. Geophys. Res.,* **99,** 14 415–14 428.

——, ——, and ——, 1996: One-dimensional statistical dynamic representation of subgrid variability of precipitation in the two-layer variable infiltration capacity model. *J. Geophys. Res.,* **101,** 21 403–21 422.

Lohmann, D., R. Nolte-Holube, and E. Raschke, 1996: A large-scale horizontal routing model to be coupled to land surface parametrization schemes. *Tellus,* **48A,** 708–721.

——, E. Raschke, B. Nijssen, and D. P. Lettenmaier, 1998: Regional scale hydrology: I. Formulation of the VIC-2L model coupled to a routing model. *Hydrol. Sci. J.,* **43,** 131–141.

Lott, N., and T. Ross, 2006: Tracking and evaluating U.S. billion dollar weather disasters, 1980–2005. Preprints, *AMS Forum: Environmental Risk and Impacts on Society: Success and Challenges,* Atlanta, GA, Amer. Meteor. Soc., 1.2. [Available online at http://ams.confex.com/ams/Annual2006/techprogram/paper_100686.htm.]

Mao, D., K. A. Cherkauer, and L. C. Bowling, 2007: Improved vegetation properties for the estimation of evapotranspiration in the Midwest United States. *ASABE Annual Int. Meeting,* Minneapolis, MN, American Society of Agricultural and Biological Engineers, 072152.

Maurer, E. P., A. W. Wood, J. C. Adam, D. P. Lettenmaier, and B. Nijssen, 2002: A long-term hydrologically based data set of land surface fluxes and states for the conterminous United States. *J. Climate,* **15,** 3237–3251.

McKee, T. B. N., J. Doesken, and J. Kleist, 1993: The relationship of drought frequency and duration to time scales. Preprints, *Eighth Conf. on Applied Climatology,* Anaheim, CA, Amer. Meteor. Soc., Washington, DC, 179–184.

——, ——, and ——, 1995: Drought monitoring with multiple time scales. Preprints, *Ninth Conf. on Applied Climatology,* Dallas, TX, Amer. Meteor. Soc., 233–236.

Meng, L., and S. M. Quiring, 2008: A comparison of soil moisture models using soil climate analysis network observations. *J. Hydrometeor.,* **9,** 641–659.

Mitchell, K. E., and Coauthors, 2004: The multi-institution North American Land Data Assimilation System (NLDAS): Utilizing multiple GCIP products and partners in a continental distributed hydrological modeling system. *J. Geophys. Res.,* **109,** D07S90, doi:10.1029/2003JD003823.

Mo, K. C., 2008: Model-based drought indices over the United States. *J. Hydrometeor.,* **9,** 1212–1230.

Myneni, R. B., R. R. Nemani, and S. W. Running, 1997: Estimation of global leaf area index and absorbed par using radiative transfer models. *IEEE Trans. Geosci. Remote Sens.,* **35,** 1380–1393.

Nakićenović, N., and Coauthors, 2000: Summary for policymakers. *IPCC Special Report: Emissions Scenarios,* N. Nakićenović and R. Swart, Eds., Cambridge University Press, 27 pp.

Nash, J. E., and J. V. Sutcliffe, 1970: River flow forecasting through conceptual models part I — A discussion of principles. *J. Hydrol.,* **10,** 282–290.

Nijssen, B., D. P. Lettenmaier, X. Liang, S. W. Wetzel, and E. F. Wood, 1997: Streamflow simulation for continental-scale river basins. *Water Resour. Res.,* **33,** 711–724.

——, G. M. O'Donnell, A. F. Hamlet, and D. P. Lettenmaier, 2001: Hydrologic sensitivity of global rivers to climate change. *Climatic Change,* **50,** 143–175.

Oleson, K. W., and Coauthors, 2008: Improvements to the Community Land Model and their impact on the hydrological cycle. *J. Geophys. Res.,* **113,** G01021, doi:10.1029/2007JG000563.

Regonda, S. K., B. Rajgopalan, M. Clark, and J. Pitlick, 2005: Seasonal cycles shifts in hydroclimatology over the western United States. *J. Climate,* **18,** 372–384.

Riebsame, W. E., S. A. Changnon, and T. R. Karl, 1991: *Drought and Natural Resources Management in the United States: Impacts and Implications of the 1987-89 Drought*. Westview Press, 174 pp.

Robock, A., K. Y. Vinnikov, G. Srinivasan, J. K. Entin, S. E. Hollinger, N. A. Speranskaya, S. Liu, and A. Namkhai, 2000: The Global Soil Moisture Data Bank. *Bull. Amer. Meteor. Soc.,* **81,** 1281–1299.

——, and Coauthors, 2003: Evaluation of the North American Land Data Assimilation System over the southern Great Plains during the warm season. *J. Geophys. Res.,* **108,** 8846, doi:10.1029/2002JD003245.

Schaake, J. C., and Coauthors, 2004: An intercomparison of soil moisture fields in the North American Land Data Assimilation System (NLDAS). *J. Geophys. Res.,* **109,** D01S90, doi:10.1029/2002JD003309.

Sheffield, J., and E. Wood, 2007: Characteristics of global and regional drought, 1950–2000: Analysis of soil moisture data from off-line simulation of the terrestrial hydrologic cycle. *J. Geophys. Res.,* **112,** D17115, doi:10.1029/2006JD008288.

——, and ——, 2008: Projected changes in drought occurrence under future global warming from multi-model, multi-scenario, IPCC AR4 simulations. *Climate Dyn.,* **31,** 79–105.

——, G. Goteti, F. Wen, and E. F. Wood, 2004: A simulated soil moisture based drought analysis for the United States. *J. Geophys. Res.,* **109,** D24108, doi:10.1029/2004JD005182.

Shukla, S., and A. W. Wood, 2008: Use of a standardized runoff index for characterizing hydrologic drought. *Geophys. Res. Lett.,* **35,** L02405, doi:10.1029/2007GL032487.

Sinha, T., and K. A. Cherkauer, 2008: Time series analysis of soil freeze and thaw processes in Indiana. *J. Hydrometeor.,* **9,** 936–950.

——, ——, and V. Mishra, 2010: Impacts of historic climate variability on seasonal soil frost in the midwestern United States. *J. Hydrometeor.,* in press.

Stewart, I. T., D. R. Cayan, and M. D. Dettinger, 2005: Changes toward earlier streamflow timing across western North America. *J. Climate,* **18,** 1136–1155.

Svoboda, M., and Coauthors, 2002: The Drought Monitor. *Bull. Amer. Meteor. Soc.,* **83,** 1181–1190.

Wang, A., T. J. Bohn, S. P. Mahanama, R. D. Koster, and D. P. Lettenmaier, 2009: Multimodel ensemble reconstruction of drought over the continental United States. *J. Climate,* **22,** 2694–2712.

Wilhite, D. A., M. V. K. Sivakumar, and D. A. Wood, Eds., 2000: Early warning systems for drought preparedness and drought management. World Meteorological Organization Tech. Doc. 1037, 185 pp.

WMO, 2005: Statement on the status of the global climate in 2005. WMO Rep. 998, 12 pp. [Available online at http://www.wmo.ch/index-en.html.]

Wood, A. W., E. P. Maurer, A. Kumar, and D. P. Lettenmaier, 2002: Long-range experimental hydrologic forecasting for the eastern United States. *J. Geophys. Res.,* **107,** 4429, doi:10.1029/2001JD000659.

——, L. R. Leung, V. Sridhar, and D. P. Lettenmaier, 2004: Hydrologic implications of dynamical and statistical approaches to downscaling climate model outputs. *Climatic Change,* **62,** 189–216.

Wood, E. F., D. Lettenmaier, X. Liang, B. Nijssen, and S. W. Wetzel, 1997: Hydrological Modeling of Continental-Scale Basins. *Annu. Rev. Earth Planet. Sci.,* **25,** 279–300.

Wuebbles, D. J., and K. Hayhoe, 2004: Climate Change Projections for the United States Midwest. *Mitigation Adapt. Strategies Global Change,* **9,** 335–363.

Yue, S., and C. Y. Wang, 2002: Regional streamflow trend detection with consideration of both temporal and spatial correlation. *Int. J. Climatol.,* **22,** 933–946.